schizophrenia score (PSS), which was calculated by combining the additive effects of thousands of common independent SNPs weakly associated with schizophrenia explained approximately 3% of the variance in liability for schizophrenia in independent subjects (Purcell et al., 2009). A recent study found that PSS predicts the total brain (TB) and white matter volumes (WM) but not the GM, explaining approximately 5% of the variance in the TB and WM (Terwisscha van Scheltinga et al., 2013). However, it remains unclear whether PSS affects variation in specific GM. Therefore, we investigated the effect of PSS on GM, using (i) voxel-based morphometry (VBM) and (ii) VBM-based region of interest (ROI) methods.

For PSS, the odds ratios for genome-wide SNP data were calculated in a discovery Japanese genome-wide association study (JPN_GWAS) sample including 560 patients with schizophrenia and 548 healthy subjects (Ikeda et al., 2011). On the basis of the genomic-control adjusted *p*-values in an allele-wise association analysis from the discovery sample, nominally associated alleles at the following liberal significance threshold (P_T) were selected: $P_T \leq .1$, $P_T \leq .2$, $P_T \leq .3$, $P_T \leq .4$, and $P_T \leq .5$. Of 67,315 independent SNPs remained after pruning, the numbers of SNPs at each P_T are as follows; $P_T \leq .1$ (n = 7,332), $P_T \leq .2$ (n = 14,294), $P_T \leq .3$ (n = 21,205), $P_T \leq .4$ (n = 27,921), and $P_T \leq .5$ (n = 34,523). These data were used to calculate individual PSSs in our target sample of 160 patients with schizophrenia and 378 healthy subjects. The structural images in the target sample were acquired using a 1.5T GE Magnetic Resonance Imaging (MRI) scanner, and the MRI images were processed using the VBM8 toolbox in Statistical Parametric Mapping 8 (SPM8). Detailed information regarding the subjects and methods is provided in the Supplementary Materials and Methods and Table S1. Written informed consent was obtained from all subjects after the procedures had been fully explained. This study was performed in accordance with the World Medical Association's Declaration of Helsinki and was approved by the Research Ethical Committee of Osaka University.

First, to identify brain regions related to PSS based on each threshold, we conducted a whole-brain search in patients with schizophrenia and healthy subjects using a multiple regression model in SPM8. Age, gender and diagnosis were included as covariates. As we found a marginal interaction between diagnosis and PSS on the left superior temporal gyrus (STG), an area of the brain reported to have reduced GM in high-risk individuals and first-episode and chronic schizophrenia patients (Chan et al., 2011) (a maximum of T = 4.44 and P_{FWE} = .075 at $P_T \leq .5$) (Fig. S1), we next performed separate whole-brain searches to examine the effects of PSS in patients with schizophrenia and healthy subjects. In the patients, PSS was significantly negatively correlated with the local GM in the left STG at the different P_T-values at the whole-brain corrected level ($P_{FWE} < .05$, a maximum of T = 5.04 and P_{FWE} = .012 at $P_T \leq .3$) (Fig. 1). Higher PSSs were associated with smaller left STG volumes. The STG was the only region showing the association. Such effects were similarly found at the $P_T \leq .2$ (T = 4.75, P_{FWE} = .037) to $P_T \leq .5$ (T = 4.73, P_{FWE} = .040) threshold levels, indicating that many more SNPs based on threshold levels more lenient than $P_T \leq .2$ are predictive of

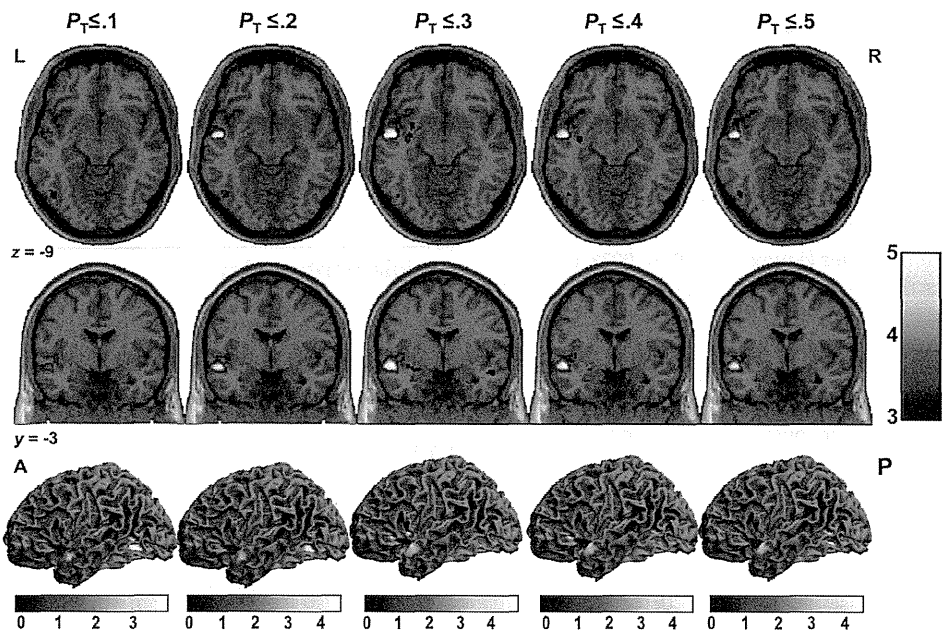

Fig. 1 – Impacts of polygenic scores on gray matter volume in patients with schizophrenia. The effects of PSS based on each threshold ($P_T \leq .1$, $P_T \leq .2$, $P_T \leq .3$, $P_T \leq .4$, and $P_T \leq .5$) on the gray matter volume are shown according to the *t* values showed by the colored bars. The most significant region of PSS association was in the left superior temporal gyrus (Talairach coordinates of peak voxel: −50, −3, −9). The anatomical localizations are displayed on the axial (upper line) and coronal (middle line) sections of a normal MRI spatially normalized to the Montreal Neurological Institute template. Z and y represent the z and y coordinates in Talairach space. The surface-rendered view (lower line) of the brain region correlating with PSS is shown. L, left; R, right; A, anterior; P, posterior.

reduced STG volumes. When including the number of nonmissing SNPs, PANSS scores, duration of illness, or antipsychotic dosage as covariates in the VBM analysis, the effects of PSS on the region remained significant ($P_{FWE} < .05$). In contrast, there was no effect of the score on the GM in healthy subjects ($P_{FWE} > .05$).

The STG is involved in auditory processing, the perception of emotions in facial stimuli, and social cognition (Bigler et al., 2007; Radua et al., 2010). To confirm whether the effect at voxel level on the initial VBM analyses is accepted in the larger structural and functional region, we secondly investigated the effects of PSS on calculated total left STG volumes in patients with schizophrenia and healthy subjects using a multiple linear regression model, with the number of nonmissing SNPs as a covariate using PASW18.0 software. Consistent with the VBM results and expected from them, the ROI analysis revealed that the PSS were significantly negatively correlated with the total left STG volume at all different P_T-values (a maximum $R^2 = .032$, $p = .0090$, at $P_T \leq .2$) in the patients (Fig. S2), whereas there was no effect of the score on the region in the controls ($p > .13$). The PSS explained approximately 3.2% of the variance in the total left STG in the patients with schizophrenia, and the effects of PSS on the region reached a peak at $P_T \leq .3$ in the VBM and $P_T \leq .2$ in the ROI analyses. To examine whether there is a strong association of SNPs with the total left STG, we subsequently conducted a GWAS of the region in the same target samples of patients with schizophrenia. We did not observe any association at a widely used benchmark for genome-wide significance ($p > 5.0 \times 10^{-8}$, Figs. S3–S4 and Table S2).

Although Ikeda et al. (2011) reported that there was a significant correlation of the PSSs between the Japanese and UK samples, there are likely many unique risk variants included in the PSS derived in the Japanese dataset. As the genes comprising the PSS in this study are not identical to those in the MRI study of Terwisscha van Scheltinga et al. (2013), we additionally attempted to replicate the association between PSS and TB and WM (Fig. S5). The PSS were marginally negatively correlated with the TB at the $P_T \leq .5$ ($R^2 = .0035$, $p = .049$) and GM at different P_T-values (a maximum $R^2 = .0073$, $p = .015$, at $P_T \leq .5$), whereas there was no effect of the score on the WM ($p > .05$). The reason why we failed to replicate the associations may be caused by false-negative results due to a small number of discovery samples and/or difference of ethnicities between present and previous studies. We used liberal thresholds ($P_T = .1$ to .5) to obtain PSS according to prior studies (Ikeda et al., 2011; Purcell et al., 2009). However, it was more liberal compared to previous study of Terwisscha van Scheltinga et al. (2013) ($P_T = .002$ to .4). The thresholds we used were so liberal as to likely include a large number of false positives.

Substantially larger controls participated in this study. However, there was a lack of the association in the group. As demographic variables in our samples did not match between healthy subjects and patients with schizophrenia, we matched controls to patients for age and sex and additionally performed the VBM analysis, by removing healthy subjects from the total samples. However, the lack of association in the control group did not change. We considered two reasons for the lack of association; 1) The PSS may be related to a genetic architecture of patients with schizophrenia but not controls because the PSS were scores derived from risk of schizophrenia. 2) The association that we detected in patients may result from a false-positive finding due to small samples.

Our findings suggest that a set of SNPs weakly associated with schizophrenia may have an accumulative effect on the brain structure of patients, but not controls. However, our findings should be carefully interpreted because there has not been enough evidence for the heritability of brain structures in unaffected siblings (Birnbaum & Weinberger, 2013). It is interesting to note that the STG is the only brain region showing significant association with the PSS in our schizophrenia dataset, even though structural imaging studies of patients with schizophrenia have identified other brain regions that show volume differences between patients and controls, and that no associations were found in normal subjects, a considerably larger sample. This selective association with the STG and only in the patients was not expected and must be viewed as preliminary pending further replication.

Acknowledgments

The authors report no conflict of interest. We would like to thank all the individuals who participated in this study. This work was supported by research grants from the Japanese Ministry of Health, Labor and Welfare (H22-seishin-ippan-001), KAKENHI, 22390225-Grant-in-Aid for Scientific Research (B), 23659565-Grant-in-Aid for Challenging Exploratory Research and Grant-in-Aid for Scientific Research on Innovative Areas (Comprehensive Brain Science Network) from the Japanese Ministry of Education, Culture, Sports, Science and Technology (MEXT), and the Japan Foundation for Neuroscience and Mental Health. The authors declare no competing financial interests.

Supplementary data

Supplementary data related to this article can be found at http://dx.doi.org/10.1016/j.cortex.2014.05.011.

REFERENCES

Bigler, E. D., Mortensen, S., Neeley, E. S., Ozonoff, S., Krasny, L., Johnson, M., et al. (2007). Superior temporal gyrus, language function, and autism. *Developmental Neuropsychology, 31*, 217–238.

Birnbaum, R., & Weinberger, D. R. (2013). Functional neuroimaging and schizophrenia: a view towards effective connectivity modeling and polygenic risk. *Dialogues in Clinical Neuroscience, 15*, 279–289.

Chan, R. C., Di, X., McAlonan, G. M., & Gong, Q. Y. (2011). Brain anatomical abnormalities in high-risk individuals, first-episode, and chronic schizophrenia: an activation likelihood estimation meta-analysis of illness progression. *Schizophrenia Bulletin, 37*, 177–188.

Ikeda, M., Aleksic, B., Kinoshita, Y., Okochi, T., Kawashima, K., Kushima, I., et al. (2011). Genome-wide association study of schizophrenia in a Japanese population. *Biological Psychiatry, 69*, 472–478.

Purcell, S. M., Wray, N. R., Stone, J. L., Visscher, P. M., O'Donovan, M. C., Sullivan, P. F., et al. (2009). Common polygenic variation contributes to risk of schizophrenia and bipolar disorder. *Nature, 460*, 748–752.

Radua, J., Phillips, M. L., Russell, T., Lawrence, N., Marshall, N., Kalidindi, S., et al. (2010). Neural response to specific components of fearful faces in healthy and schizophrenic adults. *NeuroImage, 49*, 939–946.

Sullivan, P. F., Kendler, K. S., & Neale, M. C. (2003). Schizophrenia as a complex trait: evidence from a meta-analysis of twin studies. *Archives of General Psychiatry, 60*, 1187–1192.

Terwisscha van Scheltinga, A. F., Bakker, S. C., van Haren, N. E., Derks, E. M., Buizer-Voskamp, J. E., Boos, H. B., et al. (2013). Genetic schizophrenia risk variants jointly modulate total brain and white matter volume. *Biological Psychiatry, 73*, 525–531.

Thompson, P. M., Cannon, T. D., Narr, K. L., van Erp, T., Poutanen, V. P., Huttunen, M., et al. (2001). Genetic influences on brain structure. *Nature Neuroscience, 4*, 1253–1258.

OPEN ACCESS Freely available online

PLOS | ONE

Neuromelanin Magnetic Resonance Imaging Reveals Increased Dopaminergic Neuron Activity in the Substantia Nigra of Patients with Schizophrenia

Yoshiyuki Watanabe[1]*, Hisashi Tanaka[1], Akio Tsukabe[1], Yuki Kunitomi[1], Mitsuo Nishizawa[1], Ryota Hashimoto[2,4], Hidenaga Yamamori[4], Michiko Fujimoto[4], Masaki Fukunaga[3], Noriyuki Tomiyama[1]

1 Diagnostic and Interventional Radiology, Osaka University Graduate School of Medicine, Suita, Japan, **2** Research Center for Children's Mental Development, United Graduate School of Child Development, Osaka University, Suita, Japan, **3** Departments of Biofunctional Imaging and Immunology, Frontier Research Center, Osaka University, Suita, Japan, **4** Department of Psychiatry, Osaka University Graduate School of Medicine, Suita, Japan

Abstract

Purpose: The dopamine hypothesis suggests that excessive dopamine release results in the symptoms of schizophrenia. The purpose of this study was to elucidate the dopaminergic and noradrenergic neurons using 3-T neuromelanin magnetic resonance imaging (MRI) in patients with schizophrenia and healthy control subjects.

Methods: We prospectively examined 52 patients with schizophrenia (M: F = 27:25, mean age, 35 years) and age- and sex-matched healthy controls. Using a 3T MRI unit, we obtained oblique T1-weighted axial images perpendicular to the brainstem. We measured the signal intensity and area for the substantia nigra (SNc), midbrain tegmentum, locus ceruleus (LC), and pons. We then calculated the contrast ratios (CR) for the SNc (CR_{SN}) and LC (CR_{LC}), which were compared between patients and healthy controls using unpaired *t*-tests.

Results: The SNc and LC were readily identified in both patients and healthy controls as areas with high signal intensities in the posterior part of the cerebral peduncle and in the upper pontine tegmentum. The CR_{SN} values in patients were significantly higher than those in healthy controls (10.89 ± 2.37 vs. 9.6 ± 2.36, $p<0.01$). We observed no difference in the CR_{LC} values between the patients and healthy controls (14.21 ± 3.5 vs. 13.44 ± 3.37, $p = 0.25$). Furthermore, there was no difference in area of the SNc and LC between schizophrenia patients and controls.

Conclusions: Neuromelanin MRI might reveal increased signal intensity in the SNc of patients with schizophrenia. Our results indicate the presence of excessive dopamine products in the SNc of these patients.

Citation: Watanabe Y, Tanaka H, Tsukabe A, Kunitomi Y, Nishizawa M, et al. (2014) Neuromelanin Magnetic Resonance Imaging Reveals Increased Dopaminergic Neuron Activity in the Substantia Nigra of Patients with Schizophrenia. PLoS ONE 9(8): e104619. doi:10.1371/journal.pone.0104619

Editor: Juan Zhou, Duke-NUS Graduate Medical School, Singapore

Received February 14, 2014; **Accepted** July 15, 2014; **Published** August 11, 2014

Funding: This work was supported by research grants from KAKENHI, 22390225-Grant-in-Aid for Scientific Research (B), 23659565-Grant-in-Aid for Challenging Exploratory Research and Grant-in-Aid for Scientific Research on Innovative Areas (Comprehensive Brain Science Network) from the Japanese Ministry of Education, Culture, Sports, Science and Technology (MEXT), and the Japan Foundation for Neuroscience and Mental Health. The funders had no role in study design, data collection and analysis, decision to publish, or preparation of the manuscript.

Competing Interests: One of the co-authors, Ryota Hashimoto, United Graduate School of Child Development, Osaka University, is an editor of PLOS ONE. This does not alter the authors' adherence to PLOS ONE policies on sharing data and materials.

* Email: watanabe@radiol.med.osaka-u.ac.jp

Introduction

Dopamine dysfunction plays an important role in the pathogenesis of schizophrenia [1]. The dopamine hypothesis suggests that excessive dopamine release results in symptoms of schizophrenia. *In vivo* positron emission tomography (PET) studies in patients with schizophrenia have indicated an increased baseline occupancy of D2 receptors by dopamine [2] and an increased capacity for striatal dopamine synthesis [3]. However, PET is not widely available, and its use in research is limited because of its high production costs. Further, the short half-life of ^{11}C radiopharmaceuticals restricts their use to only institutions having a cyclotron on-site.

Neuromelanin is a byproduct of the synthesis of monoamine neurotransmitters, such as noradrenalin and dopamine, and is mainly distributed within neurons of the substantia nigra (SNc) or locus ceruleus (LC) [4]. Neuromelanin has a T1-shortening effect, which was a similar characteristic of the cutaneous melanin. High-field magnetic resonance imaging (MRI), such as 3 T, is very sensitive to tissue T1 relaxation and are able to depict tissue containing neuromelanin in (SNc) or (LC) [5]. There are many previous reports which showed the signal decrease in Parkinson's disease using neuromelanin MRI [4,6–10], but there are only two reports using this technique for schizophrenia [11,12].

The purpose of this study was to use 3T neuromelanin MRI for examining dopaminergic and noradrenergic nuclei in patients with schizophrenia and healthy controls.

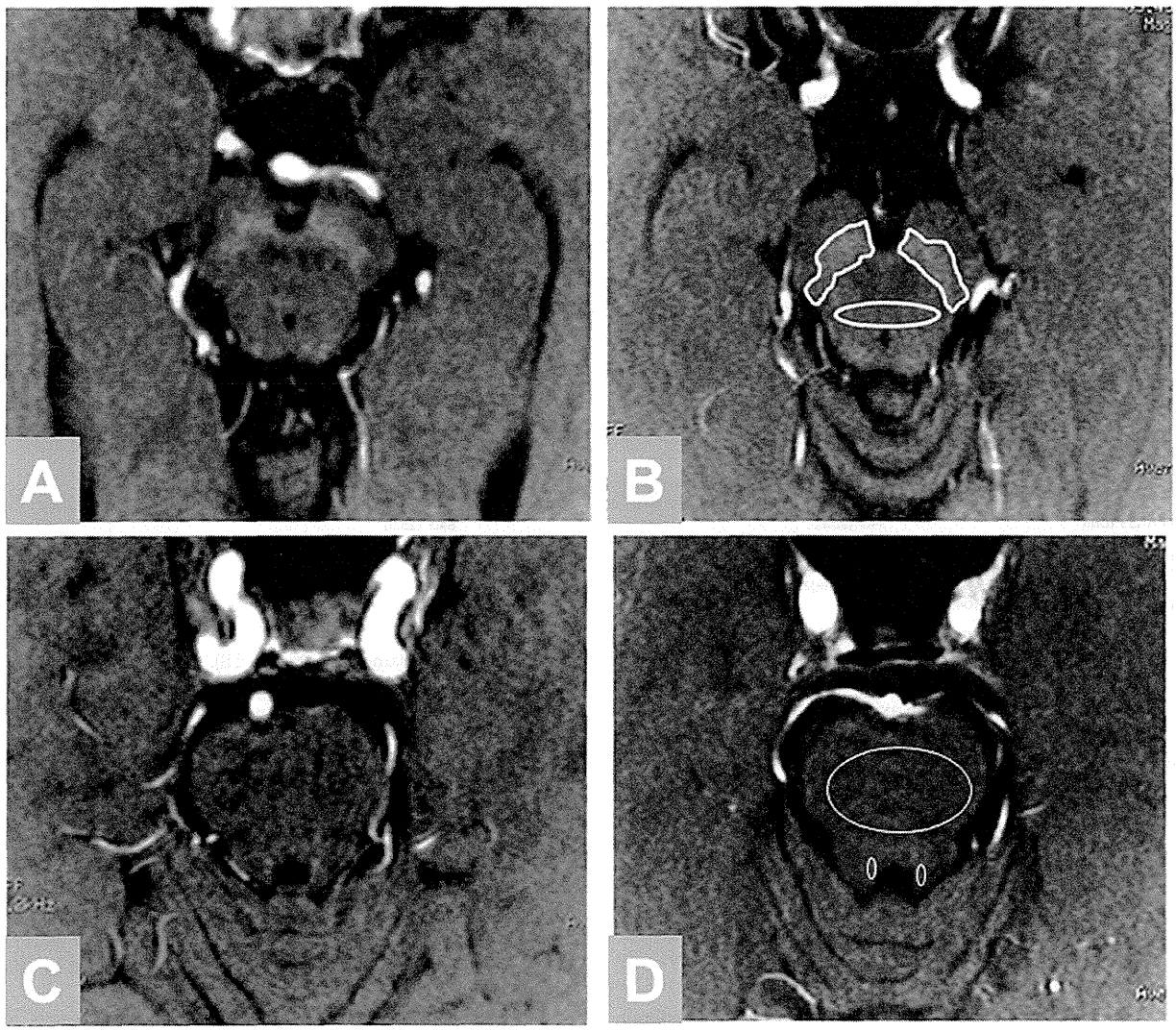

Figure 1. Neuromelanin imaging in the midbrain. A, C: 30-year-old male with schizophrenia, $CR_{SN}=12.9$, $CR_{LC}=10.7$; B, D: 26-year-old female healthy control, $CR_{SN}=6.2$, $CR_{LC}=7.6$ Demonstrating a region of interest drawn around the substantia nigra and midbrain tegmentum side on Figure 1B and locus ceruleus on Figure 1D.
doi:10.1371/journal.pone.0104619.g001

Materials and Methods

Subjects

From April to November 2012, we prospectively examined 63 consecutive patients with schizophrenia who met the *Diagnostic and Statistical Manual of Mental Disorders, 4th Edition*, (DSM-IV) diagnostic criteria using 3T-MRI. Eleven patients were excluded because of motion artifacts (6 patients) and equipment failure (5 patients). Therefore, 52 patients (M: F = 27:25; mean age = 35 years; range = 17–69 years) were included in the analysis. In addition, we obtained MRI data from age- and sex-matched healthy controls. Controls were recruited from the community through local advertisements at Osaka University. An institutional review board approved this study, and written informed consent was obtained from all subjects before their participation. We used the Japanese version of the Positive and Negative Symptom Scale (PANSS) [13] to assess patient symptoms and their severity scores. We administered the Japanese version of Wechsler Adult Intelligence Scale III [14] to determine the full scale intelligence quotient (IQ). Premorbid IQ was estimated using the Japanese Adult Reading Test [15,16].

This study was performed in accordance with the World Medical Association's Declaration of Helsinki and approved by the local institutional review board (2013-423, Osaka University Ethics Committee). Written informed consent was obtained by all subjects. If the subjects were under 20 years old, written informed consent was obtained from both minors and guardians. If the patients with schizophrenia were difficult condition to accept consent by theirself, these patients were not included in this study.

Imaging protocol

Using a 3T MRI unit (Signa Excite HDxt, GE healthcare, Milwaukee, Wisconsin), we obtained oblique T1-weighted oblique axial images perpendicular to the brainstem. The T1-weighted

Table 1. Clinical characteristics of patients with schizophrenia and healthy controls.

	Schizophrenia	Control		Schizophrenia	Control	
	all n=52	all n=52	p value	<30 year n=24	<30 year n=29	p value
Age	35.1 (13.3)	34.6 (13.7)	0.89	23.8 (4.1)	23.0 (2.3)	0.34
Sex (male:female)	27:25	27:25		11:13	16:13	
Year of education	13.4 (2.5)	15.4 (2.1)	<.001	13.0 (2.7)	15.6 (1.6)	<.001
Smoking (%)	16 (31%)	4 (7.7%)	<.001	6 (25%)	1 (3.4%)	<.001
Estimated premorbid IQ.	102.0 (10.9)	109.7 (7.3)	<.001	102.0 (11.2)	111.3 (5.0)	<.001
Full scale IQ	87.0 (20.9)	113.8 (14.1)	<.001	87.8 (20.4)	118.4 (11.4)	<.001
Age of onset	22.9 (10.1)			18.2 (3.3)		
Duration (years)	10.4 (10.9)			4.9 (4.6)		
CPZeq (mg/day)	596.2 (556.2)			495.8 (541.6)		
PANSS positive	21.0 (6.3)			18.3 (6.3)		
PANSS negative	23.1 (7.5)			20.1 (6.4)		
PANSS general	50.0 (13.9)			45.8 (13.6)		
PANSS total	94.1 (26.2)			84.1 (25.5)		

Data are shown mean (standard deviation). CPZeq: chlorpromazine equivalent of total antipsychotics.
IQ: Intelligence Quotient, PANSS: Positive and Negative Symptom Scale.
doi:10.1371/journal.pone.0104619.t001

sequence was acquired with a 3D-spoiled GRASS sequence with magnetization transfer contrast: TR/TE = 38.4/2.4 ms, FA = 20 degrees, matrix size 480×320 in axial plane, FOV = 220 mm, and acquisition time = 3 min 25 s. A 40-mm slab thickness was used and images were reconstructed 40 slices with a slice thickness of 2 mm with in-slice zero-fill interpolation (ZIP2). We also obtained axial T2-weighted images of the whole brain to exclude coexisting disorders and any abnormal findings that might influence the signals for the SNc or LC. The T2-weighted image parameters are as follows: TR/TE = 4500/88 ms, FOV = 220 mm, Matrix = 512×256, 24 slices with slice thickness 5 mm, and 6 mm slice interval.

Data analysis

We measured the signal intensity of the SNc, midbrain tegmentum, LC, and pons. The region of interest (ROI) for the SNc was traced manually around the high signal area on two consecutive axial slices and ellipse ROI was set at midbrain tegmentum in the same slice (Figure 1B). An ellipse ROI for the LC and pons were indicated on three consecutive slices. The average and maximum signal intensities (MaxSR) and area were measured for each ROI. The measurements were performed by a blinded author. We calculated the contrast ratio (CR) of the SNc (CR_{SN}) and LC (CR_{LC}) using the following equations: $CR_{SN} = (S_{SN} - S_{TM})/S_{TM}$, $CR_{LC} = (S_{LC} - S_P)/S_P$. In these equations, S_{SN} and S_{TM} are the signal intensities for the SNc and midbrain tegmentum, respectively, and S_{LC} and S_P are the signal intensities of the LC and pons, respectively.

To reduce the effects of age-related changes in the CR_{SN} and CR_{LC}, we selected a subset of subjects who were under 30 years of age (n = 24 for schizophrenia, n = 29 for healthy controls) and compared their ROI values.

Statistical analyses were performed using unpaired *t*-tests to determine the differences between patients with schizophrenia and healthy controls.

Table 2. Neuromelanin imaging characteristics of patients with schizophrenia and healthy controls.

	Schizophrenia	controls	Schizophrenia	controls	Schizophrenia	controls
	all age n=52	all age n=52	<30 years n=24	<30 years n=29	≥30 year n=28	≥30 year n=23
CR_{SN} (%)	10.89±2.37*	9.60±2.36	10.51±2.11$^{\$}$	8.85±1.95	11.22±2.80	10.55±2.51
CR_{LC} (%)	14.21±3.5	13.44±3.37	13.73±3.37	13.15±3.88	14.63±3.56	13.79±2.69
Area-SNc (mm^2)	160.1±24.1	162.2±21.6	155.4±16.9	164.8±24.7	164.2±28.1	158.9±17.1
Area-LC (mm^2)	10.84±2.46	11.42±2.27	10.79±1.93	11.67±2.57	10.89±2.82	11.09±1.86
MaxSR SNc	1.32±0.04*	1.30±0.04	1.30±0.03*	1.28±0.03	1.33±0.04	1.32±0.04
MaxSR LC	1.28±0.05	1.27±0.05	1.27±0.05	1.28±0.06	1.29±0.05	1.27±0.04

SR, signal ratio; SNc, substantia nigra; LC, locus coeruleus; CR_{SN}, contrast ratio of SNc; CR_{LC}, contrast ratio of LC;
MaxSR, maximum signal intensity.
Data are presented as mean ± standard deviation.
*p<0.05 compared to controls,
$^{\$}$p<0.005 compared to controls.
doi:10.1371/journal.pone.0104619.t002

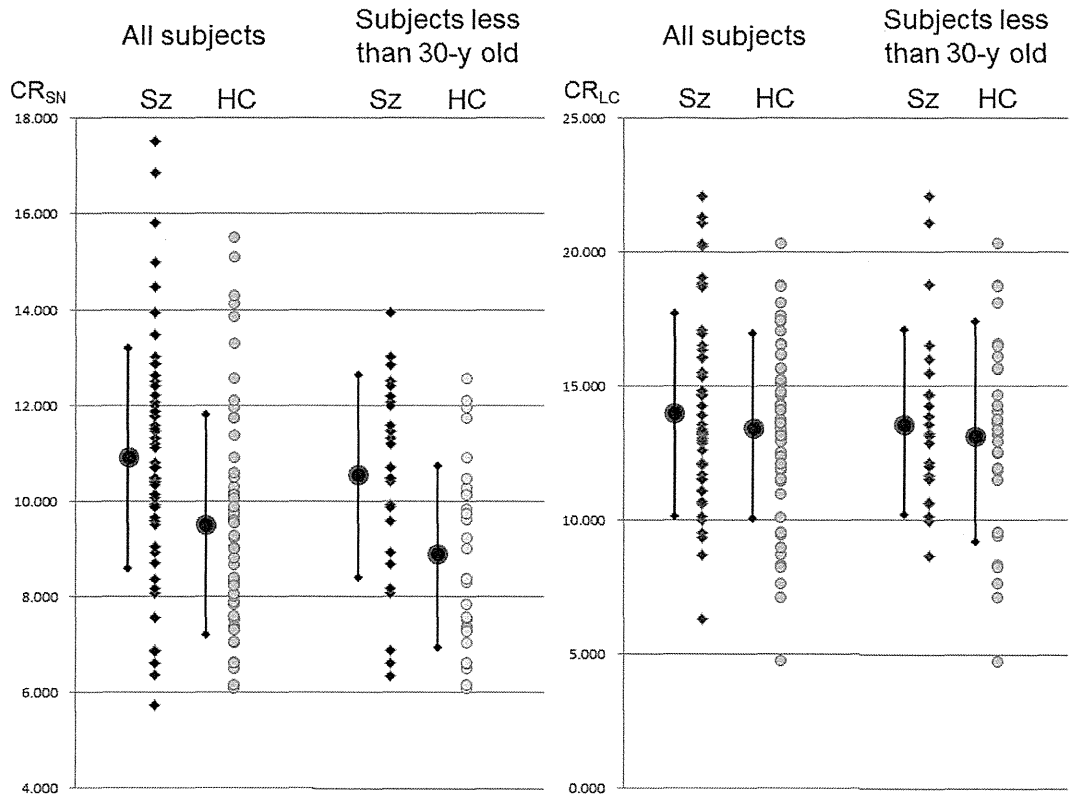

Figure 2. CR_{SN} and CR_{LC} for patients with schizophrenia and healthy controls. The left graph plots data for all subjects. The right graph plots data for selected patients under 30 years of age. The dots and bar show mean ± standard deviation. The patients showed a significantly higher CR_{SN}, but the variation in each group was large. The dispersion of data is small to select the young patients. There was no significant difference about CR_{LC} between the patients and healthy controls.
doi:10.1371/journal.pone.0104619.g002

We calculated the correlation between age and CR_{SN} or CR_{LC} for patients with schizophrenia and healthy controls. To elucidate the medication effects for the contrast ratio, the correlation between the chlorpromazine (CPZ) equivalents and CR_{SN} or CR_{LC} was analyzed.

Results

Table 1 presents the characteristics and clinical symptoms of patients and healthy controls. Compared to the patients, healthy controls had more years of education and higher IQs.

The SNc and LC were readily identified by high signal intensity areas in the posterior part of the cerebral peduncle and at the upper pontine tegmentum in both patients and healthy controls (Figure 1). Table 2 summarizes the mean signal intensities of each ROI. Our quantitative analysis showed that the CR_{SN} values and MaxSR SNc were significantly higher in patients with schizophrenia than in healthy controls (CR_{SN}: 10.89±2.37 vs. 9.6±2.36; $p<0.01$; Figure 2; MaxSR SNc: 1.32±0.04 vs. 1.30±0.04; $p<0.05$). No difference was observed in the CR_{LC} values between the patients and healthy controls (14.21±3.5 vs. 13.44±3.37; $p=0.25$; Figure 2). There was no difference the areas of the SNc and LC between schizophrenia and healthy controls.

In the subset of subjects that were under the age of 30, CR_{SN} values were significantly higher in patients with schizophrenia than in healthy controls (10.51±2.11 vs. 8.85±1.95; $p<0.005$; Figure 2). There was no significant difference for the subset of subjects over 30 years old.

There is weak correlation between age and CR_{SN} ($R=0.325$, $p=0.019$) for healthy controls and ($R=0.263$, $p=0.053$) for schizophrenia. There is no correlation between age and CR_{LC} ($R=-0.008$, $p=0.95$) for healthy controls and ($R=0.196$, $p=0.164$) for schizophrenia. The CPZ equivalent and CR_{SN} showed weak correlation ($R=0.353$, $p=0.010$) and there is no correlation between CPZ equivalent and CR_{LC} ($R=0.023$, $p=0.870$) for patients with schizophrenia.

Discussion

Our results demonstrate the excessive levels of dopamine products in the SNc of living patients with schizophrenia and this supports the dopamine hypothesis for schizophrenia. Recently, Howers et al [17] reported the same results using a post-mortem study, which revealed that tyrosine hydroxylase staining scores were significantly greater in the schizophrenia group at substantia nigra compared to in healthy controls and in vivo imaging using PET which showed that elevated dopamine synthesis was seen in the nigral dorpamine neurons in schizophrenia.

It has been suggested that dopamine dysfunction plays an important role in the pathogenesis of schizophrenia. This hypothesis is supported by evidence provided by numerous observations and studies. For example, the stimulants amphetamine and cocaine, which increase dopamine levels in the brain,

can cause symptoms resembling those for psychosis [18]. Patients with Parkinson's disease who have been treated with levodopa, a dopamine-enhancing compound, can experience psychotic adverse effects mimicking the symptoms of schizophrenia [19]. Antipsychotic drugs such as chlorpromazine, however, can antagonize dopamine D2 receptor binding and reduce the positive symptoms of psychosis [20]. Lots of in vivo studies have used PET techniques that examine receptor imaging or dopamine synthesis in order to evaluate the dopamine system in patients with schizophrenia. Dopamine D2 receptors were upregulated in patients with schizophrenia [21] and increased striatal dopamine synthesis occurs in schizophrenia [3]. However, because of low-resolution of PET, many studies evaluated at striatum and cerebral cortex.

It has been reported that T1-weighted MRI with 3T can indicate T1-shortening tissues containing neuromelanin at SNc and LC [4,5]. This technique is widely used to investigate neuromelanin signal and volume loss in the SNc of patients with Parkinson's disease [6–9,22]. We are aware of only two previous reports on neuromelanin imaging in patients with schizophrenia. Shibata et al [11] described signal changes in the SNc and LC among patients with schizophrenia, depression and controls. However, the CR_{SN} values were higher in patients with schizophrenia ($n = 20$; 22.6 ± 5.6: mean $\pm$ standard deviation (SD)) than in those with depression ($n = 18$; 19.2 ± 4.7), as well as controls ($n = 34$; 19.6 ± 3.8; one-way ANOVA, $p = 0.037$). However, a post hoc Tukey's test indicated no significant difference among schizophrenia and controls.

Sasaki et al [12] reported the CR_{SN} values were higher in patients with schizophrenia ($n = 23$; 22.6 ± 5.1) than those with depression ($n = 23$; 19.0 ± 4.3) and controls ($n = 23$; 20.5 ± 3.4). A post hoc test confirmed a significant difference between patients with schizophrenia and those with depression, but not between patients with schizophrenia and controls.

These two previous reports indicate the CR_{SN} in patients with schizophrenia is higher than that in controls, but this was not statistically significant due to a small sample size and large variations. We performed a similar comparison in our study using a lager patient group (52 patients) and observed a significant difference. The mean CR_{SN} was significantly higher in patients with schizophrenia than in healthy controls, but the CR_{SN} values showed large variations with overlap between patients and healthy controls (Figure 2). It is reported that neuromelanin levels in the SNc can increase with age using post-mortem histrogical examination [23,24] and also neuro-melanin MRI [23,25]. The age range in our study was very broad, ranging from 17 to 69 years. To reduce age-related changes, we selected subjects younger than 30 years. Between these groups, the CR_{SN} value showed small variations, and the difference between patients and healthy controls was more prominent (Figure 2).

The absolute value of CR_{SN} observed in our study differed from those in two previous reports, which likely resulted from differences of the reference ROIs and MR sequence. We used a reference ROI located in the midbrain tegmentum, whereas previous reports used the decussation of the superior cerebellar peduncle. We use 3D-SPGR sequence to obtain T1-weighted image and previous reports performed a 2D-fast spin echo sequence. 3D acquisition is superior to obtain high signal to noise ratio image in less time. We showed significant difference using short time neuromelanin imaging and this was of great advantage to exam the schizophrenic patients who were sometimes difficult to hold steady head position for long examination time in MR unit.

There are several limitations to our study. First, we included all patients examined with neuromelanin MRI from April to November 2012. Many of these patients were under treatment with antipsychotic drugs. Our results showed that there is a weak correlation between CPZ equivalent and CR_{SN}, therefor these drugs have the potential to influence neuromelanin levels. The number of participants in this study was not enough to perform subgroup analysis and further study is needed to select first episode medication-naive patients to exclude the drug effect. Second, we could not evaluate the ventral tegmental area (VTA), which is the origin of the dopaminergic cell bodies of the mesolimbic-cortical dopaminergic system, because of the difficulty in detection the border of the VTA by neuromelanin-MRI. Third, the years of education and IQ were significantly higher in healthy controls than in patients with schizophrenia. Schizophrenia is characterized by general intellectual deficits [26,27]. The estimated premorbid IQ difference between schizophrenia and normal controls is smaller compared to that of full scale IQ, but the difference is statistically significant [28,29]. Fourth, we used 3D-SPGR imaging for neuromelanin MRI and the acquisition time was 3 min 25 s. Our acquisition time is shorter than that used for 2D-fast spin echo sequences in previous studies [4,5,11,12,30] and this short acquisition might make lower signal to noise ratio and large signal variability.

In conclusion, neuromelanin MRI revealed increased signal intensity in the SNc of patients with schizophrenia. This finding indicates the presence of an excessive level of dopamine products in the SNc of these patients. Therefore, neuromelanin imaging has the potential to be useful for accurate diagnosis of schizophrenia and to serve as a surrogate marker for medication.

Author Contributions

Conceived and designed the experiments: YW NT. Performed the experiments: YW HT AT YK MN RH HY M. Fujimoto. Analyzed the data: YW M. Fukunaga. Contributed reagents/materials/analysis tools: YW M. Fukunaga. Wrote the paper: YW.

References

1. Heinz A, Schlagenhauf F (2010) Dopaminergic dysfunction in schizophrenia: salience attribution revisited. Schizophr Bull 36: 472–485.
2. Abi-Dargham A, Rodenhiser J, Printz D, Zea-Ponce Y, Gil R, et al. (2000) Increased baseline occupancy of D2 receptors by dopamine in schizophrenia. Proc Natl Acad Sci U S A 97: 8104–8109.
3. Hietala J, Syvalahti E, Vuorio K, Rakkolainen V, Bergman J, et al. (1995) Presynaptic dopamine function in striatum of neuroleptic-naive schizophrenic patients. Lancet 346: 1130–1131.
4. Sasaki M, Shibata E, Tohyama K, Takahashi J, Otsuka K, et al. (2006) Neuromelanin magnetic resonance imaging of locus ceruleus and substantia nigra in Parkinson's disease. Neuroreport 17: 1215–1218.
5. Sasaki M, Shibata E, Tohyama K, Kudo K, Endoh J, et al. (2008) Monoamine neurons in the human brain stem: anatomy, magnetic resonance imaging findings, and clinical implications. Neuroreport 19: 1649–1654.
6. Kashihara K, Shinya T, Higaki F (2011) Neuromelanin magnetic resonance imaging of nigral volume loss in patients with Parkinson's disease. J Clin Neurosci 18: 1093–1096.
7. Schwarz ST, Rittman T, Gontu V, Morgan PS, Bajaj N, et al. (2011) T1-weighted MRI shows stage-dependent substantia nigra signal loss in Parkinson's disease. Mov Disord 26: 1633–1638.
8. Lehericy S, Sharman MA, Dos Santos CL, Paquin R, Gallea C (2012) Magnetic resonance imaging of the substantia nigra in Parkinson's disease. Mov Disord 27: 822–830.
9. Matsuura K, Maeda M, Yata K, Ichiba Y, Yamaguchi T, et al. (2013) Neuromelanin magnetic resonance imaging in Parkinson's disease and multiple system atrophy. Eur Neurol 70: 70–77.
10. Ohtsuka C, Sasaki M, Konno K, Koide M, Kato K, et al. (2013) Changes in substantia nigra and locus coeruleus in patients with early-stage Parkinson's disease using neuromelanin-sensitive MR imaging. Neurosci Lett 541: 93–98.

11. Shibata E, Sasaki M, Tohyama K, Otsuka K, Endoh J, et al. (2008) Use of neuromelanin-sensitive MRI to distinguish schizophrenic and depressive patients and healthy individuals based on signal alterations in the substantia nigra and locus ceruleus. Biol Psychiatry 64: 401–406.
12. Sasaki M, Shibata E, Ohtsuka K, Endoh J, Kudo K, et al. (2010) Visual discrimination among patients with depression and schizophrenia and healthy individuals using semiquantitative color-coded fast spin-echo T1-weighted magnetic resonance imaging. Neuroradiology 52: 83–89.
13. Kay SR, Fiszbein A, Opler LA (1987) The positive and negative syndrome scale (PANSS) for schizophrenia. Schizophr Bull 13: 261–276.
14. Committee JW-IP (2006) Japanese Wechsler Adult Intelegence Scale Third Edition. Tokyo: Nihon Bunka Kagakusha.
15. Ota T, Iida J, Sawada M, Suehiro Y, Kishimoto N, et al. (2013) Comparison of pervasive developmental disorder and schizophrenia by the Japanese version of the National Adult Reading Test. Int J Psychiatry Clin Pract 17: 10–15.
16. Matsuoka K, Uno M, Kasai K, Koyama K, Kim Y (2006) Estimation of premorbid IQ in individuals with Alzheimer's disease using Japanese ideographic script (Kanji) compound words: Japanese version of National Adult Reading Test. Psychiatry Clin Neurosci 60: 332–339.
17. Howes OD, Williams M, Ibrahim K, Leung G, Egerton A, et al. (2013) Midbrain dopamine function in schizophrenia and depression: a post-mortem and positron emission tomographic imaging study. Brain 136: 3242–3251.
18. Gururajan A, Manning EE, Klug M, van den Buuse M (2012) Drugs of abuse and increased risk of psychosis development. Aust N Z J Psychiatry 46: 1120–1135.
19. Zahodne LB, Fernandez HH (2008) Pathophysiology and treatment of psychosis in Parkinson's disease: a review. Drugs Aging 25: 665–682.
20. Seeman P (2010) Dopamine D2 receptors as treatment targets in schizophrenia. Clin Schizophr Relat Psychoses 4: 56–73.
21. Wong DF, Wagner HN Jr, Tune LE, Dannals RF, Pearlson GD, et al. (1986) Positron emission tomography reveals elevated D2 dopamine receptors in drug-naive schizophrenics. Science 234: 1558–1563.
22. Ogisu K, Kudo K, Sasaki M, Sakushima K, Yabe I, et al. (2013) 3D neuromelanin-sensitive magnetic resonance imaging with semi-automated volume measurement of the substantia nigra pars compacta for diagnosis of Parkinson's disease. Neuroradiology 55: 719–724.
23. Zucca FA, Bellei C, Giannelli S, Terreni MR, Gallorini M, et al. (2006) Neuromelanin and iron in human locus coeruleus and substantia nigra during aging: consequences for neuronal vulnerability. J Neural Transm 113: 757–767.
24. Mann DM, Yates PO (1974) Lipoprotein pigments–their relationship to ageing in the human nervous system. II. The melanin content of pigmented nerve cells. Brain 97: 489–498.
25. Tanaka M, Aihara Y, Ikeda S, Aihara Y (2011) [Neuromelanin-related contrast in the substantia nigra semiquantitatively evaluated by magnetic resonance imaging at 3T: comparison between normal aging and Parkinson disease]. Rinsho Shinkeigaku 51: 14–20.
26. Bilder RM, Reiter G, Bates J, Lencz T, Szeszko P, et al. (2006) Cognitive development in schizophrenia: follow-back from the first episode. J Clin Exp Neuropsychol 28: 270–282.
27. Keefe RS, Eesley CE, Poe MP (2005) Defining a cognitive function decrement in schizophrenia. Biol Psychiatry 57: 688–691.
28. Fujino H, Sumiyoshi C, Sumiyoshi T, Yasuda Y, Yamamori H, et al. (2014) Performance on the Wechsler Adult Intelligence Scale-III in Japanese patients with schizophrenia. Psychiatry Clin Neurosci.
29. Woodberry KA, Giuliano AJ, Seidman LJ (2008) Premorbid IQ in schizophrenia: a meta-analytic review. Am J Psychiatry 165: 579–587.
30. Shibata E, Sasaki M, Tohyama K, Kanbara Y, Otsuka K, et al. (2006) Age-related changes in locus ceruleus on neuromelanin magnetic resonance imaging at 3 Tesla. Magn Reson Med Sci 5: 197–200.

OPEN

Citation: Transl Psychiatry (2014) **4**, e472; doi:10.1038/tp.2014.110

www.nature.com/tp

ORIGINAL ARTICLE

Common variants at 1p36 are associated with superior frontal gyrus volume

R Hashimoto[1,2,13], M Ikeda[3,13], F Yamashita[4], K Ohi[2], H Yamamori[2,5], Y Yasuda[2], M Fujimoto[2], M Fukunaga[6], K Nemoto[7], T Takahashi[8], M Tochigi[9], T Onitsuka[10], H Yamasue[9], K Matsuo[11], T Iidaka[12], N Iwata[3], M Suzuki[8], M Takeda[1,2], K Kasai[9] and N Ozaki[12]

The superior frontal gyrus (SFG), an area of the brain frequently found to have reduced gray matter in patients with schizophrenia, is involved in self-awareness and emotion, which are impaired in schizophrenia. However, no genome-wide association studies of SFG volume have investigated in patients with schizophrenia. To identify single-nucleotide polymorphisms (SNPs) associated with SFG volumes, we demonstrated a genome-wide association study (GWAS) of gray matter volumes in the right or left SFG of 158 patients with schizophrenia and 378 healthy subjects. We attempted to bioinformatically ascertain the potential effects of the top hit polymorphism on the expression levels of genes at the genome-wide region. We found associations between five variants on 1p36.12 and the right SFG volume at a widely used benchmark for genome-wide significance ($P < 5.0 \times 10^{-8}$). The strongest association was observed at rs4654899, an intronic SNP in the eukaryotic translation initiation factor 4 gamma, 3 (*EIF4G3*) gene on 1p36.12 ($P = 7.5 \times 10^{-9}$). No SNP with genome-wide significance was found in the volume of the left SFG ($P > 5.0 \times 10^{-8}$); however, the rs4654899 polymorphism was identified as the locus with the second strongest association with the volume of the left SFG ($P = 1.5 \times 10^{-6}$). *In silico* analyses revealed a proxy SNP of rs4654899 had effect on gene expression of two genes, *HP1BP3* lying 3′ to *EIF4G3* ($P = 7.8 \times 10^{-6}$) and *CAPN14* at 2p ($P = 6.3 \times 10^{-6}$), which are expressed in moderate-to-high levels throughout the adult human SFG. These results contribute to understand genetic architecture of a brain structure possibly linked to the pathophysiology of schizophrenia.

Translational Psychiatry (2014) **4,** e472; doi:10.1038/tp.2014.110; published online 21 October 2014

INTRODUCTION

Schizophrenia is a common and complex psychiatric disorder with a lifetime risk of approximately 1%. This disorder has a strong genetic component; the estimated heritability is 81%.[1] Multiple genetic variants that have a small effect have been implicated in the pathogenesis of schizophrenia.[2] A genome-wide association study (GWAS) of single-nucleotide polymorphisms (SNPs) that accesses tens of thousands of DNA samples from patients and controls can be a powerful tool for identifying common risk factors for complex diseases, such as schizophrenia. GWASs on schizophrenia have identified several genome-wide significant associated variants.[3,4] Subsequently, GWASs on neurobiological quantitative traits as intermediate phenotypes that possibly reflect the underlying genetic vulnerability better than diagnostic categorization, such as schizophrenia,[5,6] have been performed to minimize the clinical and genetic heterogeneity in studies of schizophrenia.[7]

The superior frontal gyrus (SFG) of the brain is frequently found to have reduced gray matter in individuals with first-episode schizophrenia and neuroleptic naive schizophrenia, as well as chronic patients with schizophrenia.[8,9] The SFG is involved in self-awareness and emotion.[10,11] Self-awareness is the cognitive ability to differentiate between self and non-self cues and is necessary to understand the behavior of other humans. Disturbance in self-awareness linked to social cognition is a core feature of schizophrenia.[12] Emotional disturbances, including meaningless laughter, are often observed in patients with schizophrenia. Meaningless laughter was also observed in unaffected siblings of schizophrenia, thus indicating its heritability.[13] In addition, laughter can be elicited by electrical stimulation of the SFG. Gray matter volumes of bilateral SFG have a strong genetic component, with an estimated heritability of 76–80%.[14] As there is considerable inter-individual variation in the degree of reduced volume of the SFG, it appears that genetic influences have a role in determining the degree of volume reduction of the SFG in schizophrenia. Although GWASs of bilateral hippocampal volume have recently been reported,[15,16] no study has investigated other brain areas in patients with schizophrenia. To identify an SNP related to SFG volumes, we conducted a GWAS of gray matter volumes in the right or left SFG of patients with schizophrenia and healthy subjects.

[1]Molecular Research Center for Children's Mental Development, United Graduate School of Child Development, Osaka University, Suita, Osaka, Japan; [2]Department of Psychiatry, Osaka University Graduate School of Medicine, Suita, Osaka, Japan; [3]Department of Psychiatry, Fujita Health University School of Medicine, Toyoake, Aichi, Japan; [4]Division of Ultrahigh Field MRI, Institute for Biomedical Sciences, Iwate Medical University, Yahaba, Iwate, Japan; [5]Department of Molecular Neuropsychiatry, Osaka University Graduate School of Medicine, Suita, Osaka, Japan; [6]Biofunctional Imaging, Immunology Frontier Research Center, Osaka University, Suita, Osaka, Japan; [7]Department of Neuropsychiatry, Institute of Clinical Medicine, University of Tsukuba, Ibaraki, Japan; [8]Department of Neuropsychiatry, Graduate School of Medicine and Pharmaceutical Sciences, University of Toyama, Toyama, Japan; [9]Department of Neuropsychiatry, Graduate School of Medicine, University of Tokyo, Tokyo, Japan; [10]Department of Neuropsychiatry, Graduate School of Medical Sciences, Kyushu University, Fukuoka, Japan; [11]Division of Neuropsychiatry, Department of Neuroscience, Yamaguchi University Graduate School of Medicine, Yamaguchi, Japan and [12]Department of Psychiatry, Nagoya University Graduate School of Medicine, Nagoya, Aichi, Japan. Correspondence: Professor R Hashimoto, Molecular Research Center for Children's Mental Development, United Graduate School of Child Development, Osaka University, D3, 2-2, Yamadaoka, Suita, Osaka 5650871, Japan.
E-mail: hashimor@psy.med.osaka-u.ac.jp
[13]These authors contributed equally to this work.
Received 3 June 2014; revised 4 August 2014; accepted 31 August 2014

MATERIALS AND METHODS

Subjects

We selected 281 patients with schizophrenia (52.0% males, 146 males and 135 females; mean age 36.0 ± 12.4 years) and 413 healthy controls (49.6% males, 205 males and 208 females; mean age 36.4 ± 12.8 years) for a GWAS of schizophrenia-related phenotypes, such as structural brain morphology, neurocognitive function and neurophysiological assessments.[17–19] All of the subjects were biologically unrelated, there were no first- or second-degree relatives, and all were of Japanese descent.[20,21] The subjects were excluded if they had neurological or medical conditions that could potentially affect the central nervous system, such as atypical headaches, head trauma with loss of consciousness, chronic lung disease, kidney disease, chronic hepatic disease, thyroid disease, active cancer, cerebrovascular disease, epilepsy, seizures, substance-related disorders or mental retardation. Patients with schizophrenia were recruited from the Osaka University Hospital. Each patient had been diagnosed by at least two trained psychiatrists according to the criteria from the DSM-IV (Diagnostic and Statistical Manual of Mental Disorders, Fourth Edition) based on the Structured Clinical Interview for DSM-IV. Current symptoms of schizophrenia were evaluated using the positive and negative syndrome scale. Controls were recruited through local advertisements at Osaka University. The healthy subjects were evaluated using the non-patient version of the Structured Clinical Interview for DSM-IV to exclude individuals who had current or past contact with psychiatric services or who had received psychiatric medications.

Superior frontal volumes obtained from the magnetic resonance imaging data were assessed in 158 patients with schizophrenia and 378 healthy subjects. Detailed demographic information is shown in Supplementary Table S1. Mean age and handedness did not differ significantly between the cases and controls ($P > 0.50$); however, the gender ratio, years of education and estimated premorbid intelligence quotient differed significantly between the cases and controls ($P < 0.05$). The ratio of male was higher in patients with schizophrenia compared with the controls. The years of education and estimated premorbid intelligence quotient were significantly lower in patients with schizophrenia compared with the controls. When the genotype groups in the top five SNPs with genome-wide significance of the right SFG volume were compared within the patient and control groups, we found no differences across the demographic variables, except for the gender ratio in the controls (rs6700718, rs1354792, rs10218584, and rs6702110; $P < 0.05$). Written informed consent was obtained from all the subjects after the procedures had been fully explained. This study was performed in accordance with the World Medical Association's Declaration of Helsinki and was approved by the Research Ethical Committee of Osaka University.

Magnetic resonance imaging procedure and extraction of SFG volumes

All magnetic resonance imaging data were obtained using a 1.5-T GE Signa EXCITE system (Tokyo, Japan). A three-dimensional volumetric acquisition of a T1-weighted gradient echo sequence produced a gapless series of 124 sagittal sections using a spoiled gradient-recalled acquisition in the steady state (SPGR) sequence (TE/TR, 4.2/12.6 ms; flip angle, 15°; acquisition matrix, 256 × 256; 1NEX, FOV, 24 × 24 cm; slice thickness, 1.4 mm). We screened all scans and found no gross abnormalities, such as infarcts, hemorrhages or brain tumors, in any of the subjects. Each image was visually examined to eliminate any images with motion or metal artifacts, and the anterior commissure–posterior commissure line was adjusted.[22] MR images were processed with the VBM8 toolbox (http://dbm.neuro.uni-jena.de/vbm/download/) implemented for SPM8 (Wellcome Department of Imaging Neuroscience, University College London, UK, http://www.fil.ion.ucl.ac.uk/spm) running in MATLAB (The Mathworks, Natick, MA, USA) for tissue segmentation and anatomical normalization, as described elsewhere.[23–25] The voxel values of the normalized gray matter images were modulated according to the nonlinear component of the transformation, which resulted in approximating brain-size-adjusted gray matter volumes while preserving local volume changes.[26] Gray matter volumes of the bilateral SFG were then calculated by using the maximum probabilistic atlas using 20 hand-labeled images (Supplementary Figure S1).[27,28]

SNP selection and SNP genotyping

Genotyping was performed using the Affymetrix Genome-Wide Human SNP Array 6.0 (Affymetrix, Santa Clara, CA, USA), according to the manufacturer's protocol. The genotypes were called from the CEL files using Birdseed v2 for the 6.0 chip implemented in the Genotyping Console software (Affymetrix). We then applied the following quality control (QC) criteria to exclude samples: (i) arrays with low QC (< 0.4) according to Birdseed v2 ($N = 0$), (ii) samples for which $< 95\%$ of the genotypes were called ($N = 0$) and (iii) samples in the same family according to $\hat{\pi}$ (> 0.4, $N = 0$). Next, we excluded SNPs that: (i) had low call rates (< 0.95), (ii) were duplicated, (iii) were localized to sex chromosomes, (iv) deviated from Hardy–Weinberg equilibrium in the controls ($P < 0.0001$) or (v) had low minor allele frequencies < 0.05. After all of these exclusions, 517 946 SNPs that underwent QC remained for experimental analysis.

To test for the existence of a genetic structure in the data, we performed a principal component analysis using EIGENSTRAT 3.0 software.[29] Ten eigenvectors were calculated. Genotype information from the JPT (Japanese in Tokyo, Japan), CHB (Han Chinese in Beijing, China), CEU (Utah residents with ancestors from northern and western Europe) and YRI (Yoruba in Ibadan, Nigeria) in HapMap phase III was compared with our data set to check for population stratification (Supplementary Figure S2).

Statistical analyses

Statistical analyses of the demographic variables were performed using PASW Statistics 18.0 software (SPSS Japan, Tokyo, Japan). Differences in the clinical characteristics between patients and controls were analyzed using χ^2 tests for the categorical variables and the Mann–Whitney *U*-test for the continuous variables. Multiple linear regression analysis was performed to compare the gray matter volumes in the right and left SFG regions among genotypes (the number of major alleles; 0, 1 or 2) using PLINK 1.07 software. Diagnosis, age and gender were included as covariates. Quantile–Quantile is listed in Supplementary Figure S3.

RESULTS

We observed associations between five variants (rs4654899, rs6702110, rs6700718, rs10218584 and rs1354792) on 1p36.12 and the right SFG volume at a widely used benchmark for genome-wide significance ($P < 5.0 \times 10^{-8}$, r^2 among SNPs > 0.8; Figure 1). The strongest association was observed at rs4654899, an intronic SNP in the eukaryotic translation initiation factor 4 gamma, 3 (*EIF4G3*) gene on 1p36.12 ($P = 7.5 \times 10^{-9}$; Figure 2). No SNP with genome-wide significance was found in the volume of the left SFG; however, the rs4654899 polymorphism was identified as the locus with the second strongest association with the volume of the left SFG ($P = 1.5 \times 10^{-6}$; Figure 1). The top 10 and top 200 markers on each SFG are shown in Tables 1 and 2 and Supplementary Tables S2 and S3. *Post hoc* analyses separately assessed in patients and controls also revealed reduced but significant associations (Tables 1 and 2 and Supplementary Tables S2 and S3). Genotype effects of rs4654899 on gray matter volume of right superior frontal gyrus were found in patients with schizophrenia and controls (Figure 3). We attempted to bioinformatically ascertain the potential effects of the rs4654899 polymorphism on the expression levels of genes at the genome-wide region by using the mRNA by SNP Browser 1.0.1 database (http://www.sph.umich.edu/csg/liang/asthma/). Significant effects of the rs3767248 proxy SNP for rs4654899 ($r^2 = 1.0$) were identified

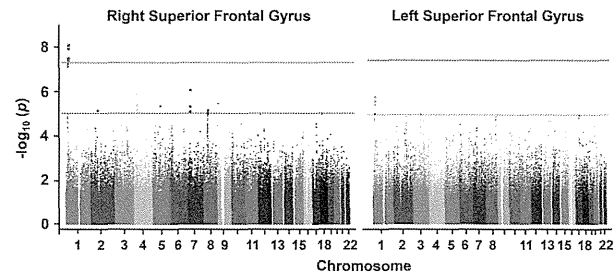

Figure 1. Manhattan plots derived from the multiple linear regression analysis of the bilateral superior frontal volumes. The blue line indicates a *P*-value of 1.0E−05. The red line indicates a *P*-value of 5.0E−08.

in the expressions of the heterochromatin protein 1, binding protein 3 (*HP1BP3*) gene ($P=7.8\times10^{-6}$), which lies 3′ to *EIF4G3*, as a cis-acting effect (< 200 kb), and the calpain 14 (*CAPN14*) gene ($P=6.3\times10^{-6}$), as a trans-acting effect (> 200 kb; Supplementary Table S4). Both *HP1BP3* and *CAPN14* are expressed in moderate-to-high levels throughout the adult human SFG (Supplementary Figures S4 and Supplementary Figure S5), as visualized in the Allen Institute Human Brain Atlas Explorer 2 software (http://human.brain-map.org/static/brainexplorer).

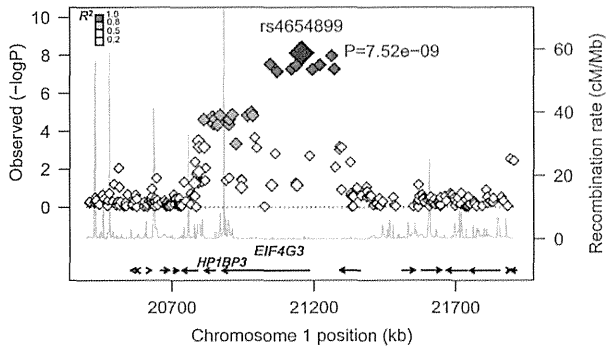

Figure 2. The strongest association with the right superior frontal gyrus was found for rs4654899. *P*-values ($-\log_{10}$) are shown in regions peripheral to rs4654899 (±750 kb).

DISCUSSION

To date, it remained unclear whether there were genetic variants strongly related to SFG volume in patients with schizophrenia and healthy subjects. This study is the first GWAS to identify the SNPs associated with the SFG, which have an important role in schizophrenia-related social functions and is reduced in patients with schizophrenia. We revealed that there were associations at the genome-wide significant level between SFG and genetic variants of the *EIF4G3* gene on 1p36.12. Individuals with minor A-allele of the most significant variant rs4654899 had smaller right SFG volumes compared with those with major C-allele in both patients and controls. Bioinformatical data indicate that the rs3767248 proxy SNP for rs4654899 has important roles in the expression of the *HP1BP3* and *CAPN14* genes, which are expressed in human adult SFG. The *HP1BP3* and *CAPN14* gene expressions of the minor G-allele of the rs3767248 polymorphism were significantly lower than those of the major A-allele. However, whether the expression levels of these genes in the brains or serums of patients with schizophrenia are lower or higher than those in healthy subjects is unknown. Further study is needed to investigate the difference of the expressions between patients and controls.

Table 1. TOP 10 SNPs for the right superior frontal gyrus

Rank	*SNP*	*Chr*	*Bp*	*m*	*M*	*MAF*	*Combined subjects*			*Schizophrenia*			*Controls*			*Closest gene*
							N	*β*	P	*N*	*β*	P	*N*	*β*	P	
1	rs4654899	1	21410231	A	C	0.33	509	−969.5	**7.52E−09**	153	−1164	3.71E−04	356	−935.9	1.86E−06	*EIF4G3*
2	rs6702110	1	21515906	G	A	0.32	526	−965.3	**1.07E−08**	155	−1255	1.79E−04	371	−902.3	4.34E−06	*EIF4G3*
3	rs6700718	1	21299363	A	C	0.33	537	−895.1	**2.89E−08**	159	−1110	4.68E−04	378	−847.7	6.81E−06	*EIF4G3*
4	rs10218584	1	21474480	G	C	0.33	537	−891.8	**3.21E−08**	159	−1110	4.68E−04	378	−842.7	7.68E−06	*EIF4G3*
5	rs1354792	1	21391875	C	T	0.33	535	−892.7	**3.46E−08**	157	−1114	5.35E−04	378	−847.7	6.81E−06	*EIF4G3*
6	rs6703227	1	21374810	C	T	0.33	537	−879.3	5.28E−08	159	−1056	9.55E−04	378	−847.7	6.81E−06	*EIF4G3*
7	rs1609558	1	21525228	C	T	0.30	533	−899.8	5.36E−08	158	−1031	1.18E−03	375	−870.9	7.67E−06	*EIF4G3*
8	rs12402486	1	21447935	A	G	0.34	527	−880.9	5.58E−08	159	−1110	4.68E−04	368	−830	1.20E−05	*EIF4G3*
9	rs2874367	1	21324491	A	C	0.33	531	−874.5	7.19E−08	157	−1092	6.24E−04	374	−829	1.25E−05	*EIF4G3*
10	rs6945071	7	26122423	G	A	0.16	537	−1035	8.46E−07	159	−1120	3.25E−03	378	−983.2	1.02E−04	*NFE2L3*

Abbreviations: Chr, chromosome; Bp, nucleotide location; m, minor allele; M, major allele; MAF, minor allele frequency; SNP, single-nucleotide polymorphism. Genome-wide significant *P*-values are shown as bold font and are underlined.

Table 2. TOP 10 SNPs for the left superior frontal gyrus

Rank	*SNP*	*Chr*	*Bp*	*m*	*M*	*MAF*	*Combined subjects*			*Schizophrenia*			*Controls*			*Closest gene*
							N	*β*	P	*N*	*β*	P	*N*	*β*	P	
1	rs4574391	4	27212223	C	T	0.25	533	−880	7.63E−07	158	−693	4.27E−02	375	−965	3.51E−06	*STIM2*
2	rs4654899	1	21410231	A	C	0.33	509	−787	1.51E−06	153	−691	3.81E−02	356	−863	4.22E−06	*EIF4G3*
3	rs2046701	4	27211040	C	A	0.25	532	−826	2.22E−06	158	−697	3.87E−02	374	−887	1.28E−05	*STIM2*
4	rs1609558	1	21525228	C	T	0.3	533	−763	2.33E−06	158	−524	1.11E−01	375	−885	1.67E−06	*EIF4G3*
5	rs6702110	1	21515906	G	A	0.32	526	−769	3.37E−06	155	−714	3.90E−02	371	−834	9.21E−06	*EIF4G3*
6	rs10218584	1	21474480	G	C	0.33	537	−704	8.32E−06	159	−566	8.48E−02	378	−791	1.05E−05	*EIF4G3*
7	rs1354792	1	21391875	C	T	0.33	535	−704	8.69E−06	157	−625	5.92E−02	378	−776	1.59E−05	*EIF4G3*
8	rs2623384	3	99064220	G	A	0.39	525	−724	9.15E−06	157	−894	6.79E−03	368	−642	5.92E−04	*COL8A1*
9	rs2292343	17	45455670	C	G	0.34	524	−721	9.74E−06	155	−836	1.22E−02	369	−666	3.45E−04	*EFCAB13*
10	rs3883317	17	45484111	A	G	0.34	534	−703	1.03E−05	158	−743	2.70E−02	376	−675	1.72E−04	*EFCAB13*

Abbreviations: Chr, chromosome; Bp, nucleotide location; m, minor allele; M, major allele; MAF, minor allele frequency; SNP, single-nucleotide polymorphism.

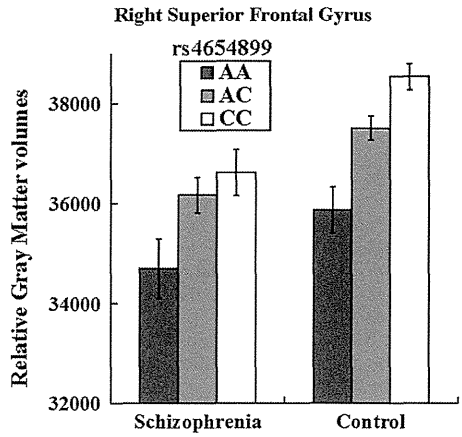

Figure 3. Impact of the rs4654899 genotype of the *EIF4G3* gene on the right superior frontal gyrus. Each column shows relative gray matter volumes of the right superior frontal gyrus. Error bars represent the standard error.

To our knowledge, no study has reported associations between these genes and schizophrenia, although the chromosomal region (1p36.12) related to the risk of schizophrenia has been reported.[30] The exact functions of these two genes are unknown; however, *HP1BP3* is predicted to bind to DNA and have a role in nucleosome assembly. *CAPN14*, which belongs to the calpain large subunit family, is a cytosolic calcium-activated cysteine protease involved in a variety of cellular processes, including apoptosis, cell division, modulation of integrin–cytoskeletal interactions and synaptic plasticity.

In this study, we examined the effects of genotypes on SFG volumes in a combined sample of patients and controls, and found similar effects of genotypes in patients and controls. Susceptibility genes for schizophrenia do not directly encode for their clinical syndrome/behaviors. The syndrome/behaviors observed in schizophrenia are produced by intermediate steps that occur between genes and syndrome/behaviors; and intermediate steps, such as changes of brain volumes, underlie the syndrome/behavior of schizophrenia. The intermediate phenotypes are located on the pathogenesis path, and are likely associated with a more basic and proximal etiological process rather than pathogenesis of disease itself.[5,6] Therefore, each genetic variant is related to controls as well as patients, and accumulations of each genetic variant could contribute to pathogenesis of schizophrenia through intermediate steps.

To date, although abnormal brain lateralization in schizophrenia causing a failure of left hemisphere dominance has been reported,[31] there is no evidence of SFG lateralization in schizophrenia. In addition, there is no report for developmental/functional differences between the right and left SFG. We found genome-wide significant variants related to right SFG volumes, whereas these variants were not related to left SFG volumes at genome-wide significant level. The difference of significance between right and left SFG was due to a difference of genotype effects in patients (for example, rs4654899, right: $P=3.71\times10^{-4}$, left: $P=3.81\times10^{-2}$) but not in controls (right: $P=1.86\times10^{-6}$, left: $P=4.22\times10^{-6}$). As it has been reported that gray matter volume deficits were more extensive in individuals with first-episode schizophrenia and neuroleptic naive than that of their neuroleptic-treated counterparts in left SFG,[9] confounding factors, such as duration of antipsychotic treatment or dose of antipsychotics, might affect our results.

In this study, we provide new insights into the genetic architecture of a brain structure closely linked to schizophrenia. It is still unclear whether and to what extent the effects of the genetic variant on SFG volumes observed here might be associated with an increased risk for schizophrenia. We suggest that the variant may have a role in the impairments of self-awareness and emotion noted in patients with schizophrenia through volumetric vulnerability of the SFG.

There were several limitations to this study. We recruited a relatively large sample with an only Japanese ethnicity to avoid population stratification. However, the existence of a false-positive association cannot be excluded as an explanation for our results. Further investigations of other samples with much larger sample sizes and/or with different ethnicities are needed to confirm our findings. It is unclear whether our results are directly/indirectly linked to the rs4654899 SNP, to other SNPs in high linkage disequilibrium with this SNP or to interactions between this SNP and other SNPs. To determine whether rs4654899 is the most strongly associated variant for SFG volume in the chromosomal region, an extensive search such as sequencing for other functional variants at this locus could provide further information underlying the genomic mechanism for this variant.

In conclusion, we found that genetic variants of the *EIF4G3* gene could be associated with structural vulnerability of the SFG. Further replication studies are necessary to confirm our findings. Identification of causal variants and the functional effects of these genes may help to reveal additional genetic variables involved in the neurodevelopment and pathogenesis of schizophrenia.

CONFLICT OF INTEREST

The authors declare no conflict of interest.

ACKNOWLEDGMENTS

We thank all the individuals who participated in this study. This work was supported by research grants from the Japanese Ministry of Health, Labor and Welfare (H22-seishin-ippan-001); KAKENHI, 22390225-Grant-in-Aid for Scientific Research (B), 23659565-Grant-in-Aid for Challenging Exploratory Research and Grant-in-Aid for Scientific Research on Innovative Areas (Comprehensive Brain Science Network) from the Japanese Ministry of Education, Culture, Sports, Science and Technology (MEXT) and the Japan Foundation for Neuroscience and Mental Health.

REFERENCES

1 Sullivan PF, Kendler KS, Neale MC. Schizophrenia as a complex trait: evidence from a meta-analysis of twin studies. *Arch Gen Psychiatry* 2003; **60**: 1187–1192.
2 Sun J, Kuo PH, Riley BP, Kendler KS, Zhao Z. Candidate genes for schizophrenia: a survey of association studies and gene ranking. *Am J Med Genet B Neuropsychiatr Genet* 2008; **147B**: 1173–1181.
3 Stefansson H, Ophoff RA, Steinberg S, Andreassen OA, Cichon S, Rujescu D *et al.* Common variants conferring risk of schizophrenia. *Nature* 2009; **460**: 744–747.
4 O'Donovan MC, Craddock N, Norton N, Williams H, Peirce T, Moskvina V *et al.* Identification of loci associated with schizophrenia by genome-wide association and follow-up. *Nat Genet* 2008; **40**: 1053–1055.
5 Meyer-Lindenberg A, Weinberger DR. Intermediate phenotypes and genetic mechanisms of psychiatric disorders. *Nat Rev Neurosci* 2006; **7**: 818–827.
6 Tan HY, Callicott JH, Weinberger DR. Intermediate phenotypes in schizophrenia genetics redux: is it a no brainer? *Mol Psychiatry* 2008; **13**: 233–238.
7 Hashimoto R, Ikeda M, Ohi K, Yasuda Y, Yamamori H, Fukumoto M *et al.* Genome-wide association study of cognitive decline in schizophrenia. *Am J Psychiatry* 2013; **170**: 683–684.
8 Chan RC, Di X, McAlonan GM, Gong QY. Brain anatomical abnormalities in high-risk individuals, first-episode, and chronic schizophrenia: an activation likelihood estimation meta-analysis of illness progression. *Schizophr Bull* 2011; **37**: 177–188.
9 Leung M, Cheung C, Yu K, Yip B, Sham P, Li Q *et al.* Gray matter in first-episode schizophrenia before and after antipsychotic drug treatment. Anatomical likelihood estimation meta-analyses with sample size weighting. *Schizophr Bull* 2011; **37**: 199–211.
10 Goldberg II, Harel M, Malach R. When the brain loses its self: prefrontal inactivation during sensorimotor processing. *Neuron* 2006; **50**: 329–339.
11 Fried I, Wilson CL, MacDonald KA, Behnke EJ. Electric current stimulates laughter. *Nature* 1998; **391**: 650.

12 Sass LA, Parnas J. Schizophrenia, consciousness, and the self. *Schizophr Bull* 2003; **29**: 427–444.
13 Bearden CE, Rosso IM, Hollister JM, Sanchez LE, Hadley T, Cannon TD. A prospective cohort study of childhood behavioral deviance and language abnormalities as predictors of adult schizophrenia. *Schizophr Bull* 2000; **26**: 395–410.
14 Hulshoff Pol HE, Schnack HG, Posthuma D, Mandl RC, Baare WF, van Oel C *et al.* Genetic contributions to human brain morphology and intelligence. *J Neurosci* 2006; **26**: 10235–10242.
15 Bis JC, DeCarli C, Smith AV, van der Lijn F, Crivello F, Fornage M *et al.* Common variants at 12q14 and 12q24 are associated with hippocampal volume. *Nat Genet* 2012; **44**: 545–551.
16 Stein JL, Medland SE, Vasquez AA, Hibar DP, Senstad RE, Winkler AM *et al.* Identification of common variants associated with human hippocampal and intracranial volumes. *Nat Genet* 2012; **44**: 552–561.
17 Hashimoto R, Ohi K, Yasuda Y, Fukumoto M, Yamamori H, Kamino K *et al.* The KCNH2 gene is associated with neurocognition and the risk of schizophrenia. *World J Biol Psychiatry* 2013; **14**: 114–120.
18 Ohi K, Hashimoto R, Yasuda Y, Nemoto K, Ohnishi T, Fukumoto M *et al.* Impact of the genome wide supported NRGN gene on anterior cingulate morphology in schizophrenia. *PLoS One* 2012; **7**: e29780.
19 Hashimoto R, Ohi K, Yasuda Y, Fukumoto M, Yamamori H, Takahashi H *et al.* Variants of the RELA gene are associated with schizophrenia and their startle responses. *Neuropsychopharmacology* 2011; **36**: 1921–1931.
20 Hashimoto R, Ohi K, Yasuda Y, Fukumoto M, Iwase M, Iike N *et al.* The impact of a genome-wide supported psychosis variant in the ZNF804A gene on memory function in schizophrenia. *Am J Med Genet B Neuropsychiatr Genet* 2010; **153B**: 1459–1464.
21 Ohi K, Hashimoto R, Yasuda Y, Fukumoto M, Nemoto K, Ohnishi T *et al.* The AKT1 gene is associated with attention and brain morphology in schizophrenia. *World J Biol Psychiatry* 2013; **14**: 100–113.
22 Evans W. An encephalographic ratio for estimating ventricular enlargement and cerebral atrophy. *Arch Neurol Psychiatry* 1942; **47**: 931–937.
23 Wilke M, Holland SK, Altaye M, Gaser C. Template-O-Matic: a toolbox for creating customized pediatric templates. *Neuroimage* 2008; **41**: 903–913.
24 Ashburner J. A fast diffeomorphic image registration algorithm. *Neuroimage* 2007; **38**: 95–113.
25 Ohi K, Hashimoto R, Yamamori H, Yasuda Y, Fujimoto M, Umeda-Yano S *et al.* The impact of the genome-wide supported variant in the cyclin M2 gene on gray matter morphology in schizophrenia. *Behav Brain Funct* 2013; **9**: 40.
26 Good CD, Johnsrude IS, Ashburner J, Henson RN, Friston KJ, Frackowiak RS. A voxel-based morphometric study of ageing in 465 normal adult human brains. *Neuroimage* 2001; **14**: 21–36.
27 Hammers A, Allom R, Koepp MJ, Free SL, Myers R, Lemieux L *et al.* Three-dimensional maximum probability atlas of the human brain, with particular reference to the temporal lobe. *Hum Brain Mapp* 2003; **19**: 224–247.
28 Heckemann RA, Hajnal JV, Aljabar P, Rueckert D. Hammers A. Automatic anatomical brain MRI segmentation combining label propagation and decision fusion. *Neuroimage* 2006; **33**: 115–126.
29 Price AL, Patterson NJ, Plenge RM, Weinblatt ME, Shadick NA, Reich D. Principal components analysis corrects for stratification in genome-wide association studies. *Nat Genet* 2006; **38**: 904–909.
30 Hong KS, Won HH, Cho EY, Jeun HO, Cho SS, Lee YS *et al.* Genome-widely significant evidence of linkage of schizophrenia to chromosomes 2p24.3 and 6q27 in an SNP-Based analysis of Korean families. *Am J Med Genet B Neuropsychiatr Genet* 2009; **150B**: 647–652.
31 Ribolsi M, Koch G, Magni V, Di Lorenzo G, Rubino IA, Siracusano A *et al.* Abnormal brain lateralization and connectivity in schizophrenia. *Rev Neurosci* 2009; **20**: 61–70.

Supplementary Information accompanies the paper on the Translational Psychiatry website (http://www.nature.com/tp)

CORTEX 63 (2015) 55–67

Available online at www.sciencedirect.com

ScienceDirect

Journal homepage: www.elsevier.com/locate/cortex

Research report

Resting state functional magnetic resonance imaging and neural network classified autism and control

Tetsuya Iidaka[*]

Department of Psychiatry, Graduate School of Medicine, Nagoya University, Nagoya, Aichi, Japan

ARTICLE INFO

Article history:
Received 3 February 2014
Reviewed 5 May 2014
Revised 2 June 2014
Accepted 12 August 2014
Action editor Mike Anderson
Published online 28 August 2014

Keywords:
Developmental disorder
Brain imaging
Diagnosis
Machine learning
Classifier

ABSTRACT

Although the neurodevelopmental and genetic underpinnings of autism spectrum disorder (ASD) have been investigated, the etiology of the disorder has remained elusive, and clinical diagnosis continues to rely on symptom-based criteria. In this study, to classify both control subjects and a large sample of patients with ASD, we used resting state functional magnetic resonance imaging (rs-fMRI) and a neural network. Imaging data from 312 subjects with ASD and 328 subjects with typical development was downloaded from the multi-center research project. Only subjects under 20 years of age were included in this analysis. Correlation matrices computed from rs-fMRI time-series data were entered into a probabilistic neural network (PNN) for classification. The PNN classified the two groups with approximately 90% accuracy (sensitivity = 92%, specificity = 87%). The accuracy of classification did not differ among the institutes, or with respect to experimental and imaging conditions, sex, handedness, or intellectual level. Medication status and degree of head movement did not affect accuracy values. The present study indicates that an intrinsic connectivity matrix produced from rs-fMRI data could yield a possible biomarker of ASD. These results support the view that altered network connectivity within the brain contributes to the neurobiology of ASD.

1. Introduction

Autism spectrum disorder (ASD) is characterized by the impaired development of social interaction and communication skills and a restricted repertoire of activities and interests (A.P.A., 1994). Although extensive efforts have been made to create a neurodevelopmental model (Baron-Cohen, 2009; Frith, 2001) and to identify disease-specific genes (Levy, Mandell, & Schultz, 2009), ASD continues to be diagnosed using symptom-based clinical criteria. The identification of biomarkers with clear neural underpinnings in ASD would be helpful in ensuring an early and accurate diagnosis as well as an optimally effective treatment (Hill & Frith, 2003; Levy et al., 2009). Structural and functional magnetic resonance imaging has the potential to reveal brain abnormalities of ASD that could be used as biomarkers of the disease.

* Department of Psychiatry, Graduate School of Medicine, Nagoya University, 65 Tsurumai, Showa, Nagoya, Aichi 466-8550, Japan.
E-mail address: iidaka@med.nagoya-u.ac.jp.
http://dx.doi.org/10.1016/j.cortex.2014.08.011
0010-9452/

A critical step in using neuroimaging abnormalities as biomarkers of ASD is applying a machine-learning algorithm such as the support vector machine (SVM) and/or an artificial neural network to the data (Orru, Pettersson-Yeo, Marquand, Sartori, & Mechelli, 2012). Structural properties of the brain, including cortical volume (Calderoni et al., 2012; Ecker, Rocha-Rego, et al., 2010; Uddin et al., 2011; Varol, Gaonkar, Erus, Schultz, & Davatzikos, 2012), thickness (Ecker, Marquand, et al., 2010; Jiao et al., 2011, 2010; Sato et al., 2013), and white matter integrity (Bloy et al., 2011; Ingalhalikar, Parker, Bloy, Roberts, & Verma, 2011), have been used as features to classify control subjects and patients with ASD; however, to date, these investigations have shown limited power of these measures as classifiers.

Investigating brain network activity during the resting state has emerged as a new method that eliminates the caveats of task-based fMRI studies (Menon, 2011). In this method, the fMRI signal is measured during the resting state and the data is analyzed based on a connectivity approach between subdivisions. To date, brain network activity during the resting state has been investigated in subjects with ASD and typical development in numerous studies (Assaf et al., 2010; Barttfeld et al., 2012; Cardinale, Shih, Fishman, Ford, & Muller, 2013; Di Martino et al., 2011; Di Martino, Zuo, et al., 2013; Ebisch et al., 2011; Lai et al., 2010; Lynch et al., 2013; Mueller et al., 2013; Murdaugh et al., 2012; Paakki et al., 2010; Tyszka, Kennedy, Paul, & Adolphs, 2014; Weng et al., 2010; Wiggins et al., 2011). Overall, intrinsic connectivity between subdivisions of the brain is altered in patients with ASD compared to controls (Muller et al., 2011; Uddin, Supekar, & Menon, 2010).

In studies that have used intrinsic connectivity during the resting state (Anderson et al., 2011; Barttfeld et al., 2012; Murdaugh et al., 2012) or during passive viewing of movies (Deshpande, Libero, Sreenivasan, Deshpande, & Kana, 2013) to classify ASD and control subjects, small sample sizes have limited the accuracy of the results. In a single study that used large samples from the same image database as the present study, the accuracy was as high as 60% (Nielsen et al., 2013). In the present study, using a large dataset (n = 640) obtained from the public database (Di Martino, Yan, et al., 2014) and a probabilistic neural network (PNN) algorithm, I report the successful classification of resting state fMRI data between subjects with ASD and subjects with typical development.

2. Materials and methods

2.1. *Materials*

The original imaging and demographic data were collected from the Autism Brain Imaging Data Exchange (ABIDE) database (http://fcon_1000.projects.nitrc.org/indi/abide/index.html), which allows unrestricted usage for non-commercial research purposes. Although the dataset included both adults and children, only subjects under 20 years of age were used in the present study. Brain images and related data from 312 subjects with ASD (male/female: 273/39) and 328 control subjects with typical development (CTL, male/female: 267/61) from 12 universities and research institutes were used. The names and abbreviations of these institutes and scanning parameters are listed in Table 1. The ethics committee of the Nagoya University School of Medicine approved the usage of this anonymous data for research purposes.

Autism was diagnosed according to both the Autism Diagnostic Interview-Revised (ADI-R) (Lord, Rutter, & Le Couteur, 1994) and the Autism Diagnostic Observation Schedule (ADOS) (Lord, Rutter, DiLavore, & Risi, 1999) in almost all cases, the exception being cases from one institute where autism was diagnosed using only the DSM-IV-TR (A.P.A., 1994). The CTL subjects were screened in clinical interviews conducted by experts in child psychiatry; however, in some cases, other questionnaires were used. The details of the diagnostic procedures and questionnaires used are listed in Supplementary Table 1.

Demographic data for each group is shown in Table 2. Subjects were aged between 6 and 19 years. The full-scale IQ of all subjects assessed was 41–148; however, no IQ data was available for three subjects with ASD. Between-group comparisons were made using unpaired t-tests (two-tailed) for age and IQ, and chi-square tests for sex and handedness (statistical threshold was set at p = .05). Data on the medication

Table 1 – Scanning parameters and experimental settings in each site.

Institute	MRI vendor	TR (msec)	TE (msec)	FA (deg)	Voxel size (mm)	Volumes	Time (m)	Eyes
KKI	Phillips	2500	30	75	3 × 3 × 3	156	6.5	o
LEU	Phillips	1667	33	90	3.48 × 3.59 × 4	250	6.9	c
NYU	Siemens	2000	15	90	3.75 × 3.75 × 4	180	6.0	o/c
OHSU	Siemens	2500	30	90	3.75 × 3.75 × 3.8	82	3.4	o
OLIN	Siemens	1500	27	60	3.43 × 3.43 × 4	210	5.3	o
PITT	Siemens	1500	25	70	3.12 × 3.12 × 4	200	5.0	c
SDSU	GE	2000	30	90	3.44 × 3.44 × 3.4	180	6.0	o
STAN	GE	2000	30	80	3.12 × 3.12 × 4.5	180	6.0	c
TRIN	Phillips	2000	28	90	3 × 3 × 3.5	150	5.0	c
UCLA	Siemens	3000	28	90	3 × 3 × 4	120	6.0	o
USM	Siemens	2000	28	90	3.43 × 3.43 × 3	240	8.0	o
YALE	Siemens	2000	25	60	3.43 × 3.43 × 4	200	6.7	o

KKI, Kennedy Krieger Institute; LEU, University of Leuven; NYU, NYU Langone Medical Center; OHSU, Oregon Health and Science University; OLIN, Olin, Institute of Living at Hartford Hospital; PITT, University of Pittsburgh School of Medicine; SDSU, San Diego State University; STAN, Stanford University; TRIN, Trinity Centre for Health Sciences; UCLA, University of California, Los Angeles; USM, University of Utah School of Medicine; YALE, Yale Child Study Center; FA; Flip angle, Time: Scan time, Eyes; eyes were open (o) or closed (c) during the scan.

Table 2 – Demographic data of the subjects.

	ASD	CTL	p-value
Number of subjects	312	328	N.A.
Mean age	13.2 (3.1)	12.9 (3.0)	.32
Male (%)	87.5	81.4	.03
Rt handedness (%)	84.3	91.8	.003
Mean full-scale IQ	103 (17)	110 (13)	.001

N.A., not available, SD in parenthesis.

status of the subjects were available from eight among the twelve sites (see Supplementary Table 2). Out of the 229 subjects with ASD investigated from these eight sites, 75 (24%) were and 152 (49%) were not receiving psychotropic medication at the time of scanning (data were not reported for two subjects). Medication status was unavailable for 83 of the ASD subjects (27%) investigated from the remaining four sites. The numbers of subjects and their demographic data from each institute are listed in Supplementary Table 2.

2.2. *Imaging data acquisition*

At each institute, functional brain images were acquired using a 3-T imager and a T2*-weighted gradient-echo echo-planar imaging (EPI) sequence, which is sensitive to blood oxygen level-dependent (BOLD) contrast. The subjects were asked to lie still in the scanner while remaining awake. Although the scanning parameters, MRI vendor, voxel size, number of volumes, scanning time, and instructions whether to keep eyes open/closed varied among the institutes, the general experimental procedure used was uniform within each institute. The number of image volumes taken for each subject ranged from 82 to 250 (mean = 179), and scanning time ranged from 3.4 min to 8.0 min (mean = 5.9 min). The details of the scanning parameters and experimental settings are provided in Table 1.

2.3. *Image data analysis*

2.3.1. *Preprocessing*

Data were analyzed using the SPM8 software (Wellcome Department of Imaging Neuroscience, London, UK, http://www.fil.ion.ucl.ac.uk/spm/) at the Department of Psychiatry, Nagoya University. After discarding the first five volumes, all volumes were spatially realigned to the mean volume, and the signal in each slice was temporally realigned to that obtained in the middle slice using sinc interpolation. The re-sliced volumes were normalized to the Montreal Neurological Institute (MNI) space with a voxel size of 3 × 3 × 3 mm^3 using an EPI template of SPM8. The normalized images were spatially smoothed with a 4-mm Gaussian kernel. Head motion is known to have substantial effects on the results for functional connectivity (Van Dijk, Sabuncu, & Buckner, 2012). The root mean square (RMS) of six movement parameters along the time-series obtained in the realignment process was calculated for each subject (x-, y-, z-translation and x-, y-, z-rotation). The RMSs of the six head movement parameters for the two groups were subjected to unpaired t-tests (two-tailed, statistical threshold at $p = .05$). The means and S.E.s of these values for each group are shown in Fig. 1.

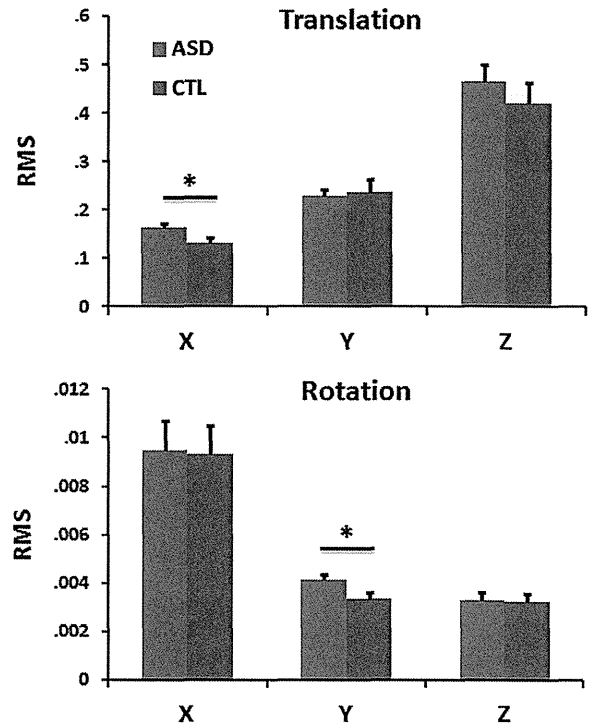

Fig. 1 – Top: The mean (column) and one S.E. (bar) of the root mean square (RMS) of translation parameters for each of the x-, y-, and z-axes obtained in the realignment process of SPM8. Blue columns represent the ASD group, and red columns represent the CTL group. There was a significant group difference in the x-axis, as indicated by a single asterisk ($p < .05$). Bottom: The mean (column) and one S.E. (bar) of the root mean square (RMS) of rotation parameters for each of the x-, y-, and z-axes obtained in the realignment process of SPM8. Blue columns represent the ASD group, and red columns represent the CTL group. There was a significant group difference in the y-axis, as indicated by a single asterisk ($p < .05$).

2.3.2. *Resting state functional connectivity analyses*

Resting state fMRI datasets were further processed using a toolkit of the Data Processing Assistant for Resting-State fMRI (DPARSF; http://www.rfmri.org) (Chao-Gan & Yu-Feng, 2010). Processing was conducted using the following steps: (1) removing the linear trend in the time series, (2) temporal band-pass filtering (.01–.08 Hz) to reduce the effect of low-frequency drift and high-frequency noise, and (3) controlling for non-neural noise in the time series by including covariates in the linear regression, i.e., six parameters from rigid body correction of head motion, the white matter signal, and the cerebrospinal fluid signal. The global mean signal was not removed in the present study (Fox, Zhang, Snyder, & Raichle, 2009; Murphy, Birn, Handwerker, Jones, & Bandettini, 2009).

Table 3 – Results of prediction accuracy: Leave-one-out cross validation.

Sensitivity	91.9%
Specificity	86.9%
Accuracy	89.4%
PPV	86.9%
NPV	91.9%
PPV_{corr}	7.4%
NPV_{corr}	99.9%

PPV, positive prediction value.
NPV, negative prediction value.
PPV_{corr}, corrected PPV.
NPV_{corr}, corrected NPV.

The residuals of the datasets after band-pass filtering and removal of the linear trend and eight covariates were considered as BOLD signal fluctuations originating from neuronal activity during the resting state. The Automated Anatomical Labeling (AAL) template (Tzourio-Mazoyer et al., 2002), which is widely used for identifying brain regions in the MNI space, was applied to the normalized and smoothed time-series datasets of each subject. The AAL template is a standard brain template for creating intrinsic connectivity (Lai et al., 2010; Supekar et al., 2013), although other templates, for example, the Harvard–Oxford Atlas (Di Martino, Yan, et al., 2014; Tyszka et al., 2014) and voxel-wise lattice method (Anderson et al., 2011; Nielsen et al., 2013) have been used for the same purpose. The AAL template divides each hemisphere into 45 distinct regions. The average time-series data were computed in each of the 90 regions for each subject. I used the AAL template because it is implemented in DPARSF software and a 90 × 90 correlation matrix is well suited to be entered into the classifier when considering the number of subjects and features. The names of these 90 regions are listed in Supplementary Table 3.

The time-series data from each of the 90 regions were cross-correlated, and Pearson's correlation coefficients (r) between each brain region and the remaining 89 regions were computed for each subject. Individuals' r values were normalized to z values using Fisher's z transformation. The z-transformed correlation coefficients were represented in a 90 × 90 matrix (8,100 cells), which was symmetric with regard to the diagonal. In the present study, the diagonal of the matrix was not valid and was not used for analysis. Therefore, the number of effective cells in the upper triangle of the matrix was 4,005. The mean and SD values of the correlation (z-transformed) matrices for the ASD and CTL groups were derived (only the mean matrices are shown in Fig. 2, left panel). Subsequently, the matrices representing the difference in mean correlation between the groups (Fig. 2, middle panel) and the standard deviation (not shown) were created. Finally, the matrix representing the effect size (Cohen's *d*) of the difference between the groups was

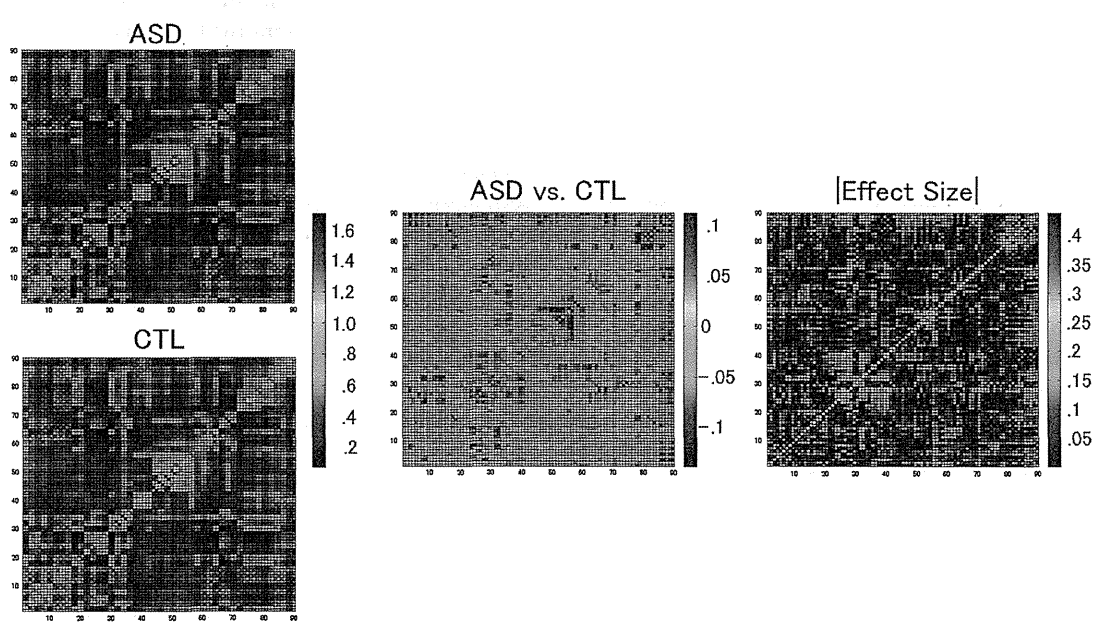

Fig. 2 – Left: Mean correlation matrices for the ASD (top, $n = 312$) and CTL (bottom, $n = 328$) groups during the resting state. The matrix represents 90 × 90 correlation coefficients of BOLD signal fluctuation between the subdivisions as defined by the AAL template. The color code indicates values of z-transformed correlation coefficients in each cell of the matrix. Middle: The difference correlation matrix between the ASD and CTL groups. The color code shows cells where subjects with ASD had greater correlations than CTL subjects in red, and cells where CTL subjects had greater correlations than subjects with ASD in blue. Right: The effect size (ES, Cohen's *d*) matrix of the difference between the ASD and CTL groups. The numerical values are absolute values. The matrix was computed from the matrices containing the differences and standard deviations of each group. The color code indicates higher ES in red and lower ES in blue. All the matrices were symmetric with respect to the diagonal, and the diagonal was invalid and was not used for analysis.

computed (Fig. 2, right panel shows matrix of absolute value of the effect size).

2.4. Classification between ASD and CTL

2.4.1. Procedure for feature selection

To search for an optimal threshold for the data to be entered into the classifier, the matrix was thresholded at seven different effect sizes (ESs, from .05 to .35 by .05 increments in absolute value). For example, at the threshold of .05 ES, 2,728 cells in the upper triangle of the matrix were used as features for the classifier. The numbers of features at each threshold are shown as columns in Fig. 3. Subsequently, z-transformed correlation coefficients of each of the 2,728 cells were extracted from the subject's original correlation matrix. The correlation data (numerical values of each cell) and diagnostic data (ASD or CTL, categorical label) were paired for each of the 640 subjects and entered into the classifier. The procedure was repeated at seven different thresholds of absolute ES.

2.4.2. PNN

A PNN (Specht, 1990) is an implementation of the kernel discriminant analysis statistical algorithm, which is organized into a multilayered feed forward neural network to perform classification. Recently, a PNN has been applied to physiological data measured by electroencephalogram (Sankari & Adeli, 2011; Ubeyli, 2008), pulse oximetry (Morillo & Gross, 2013), neuroimaging (Palumbo et al., 2010), and endoscopy (Pan, Yan, Qiu, & Cui, 2011), and has been successfully used in the classification of sample data into diseased and healthy states with high accuracy.

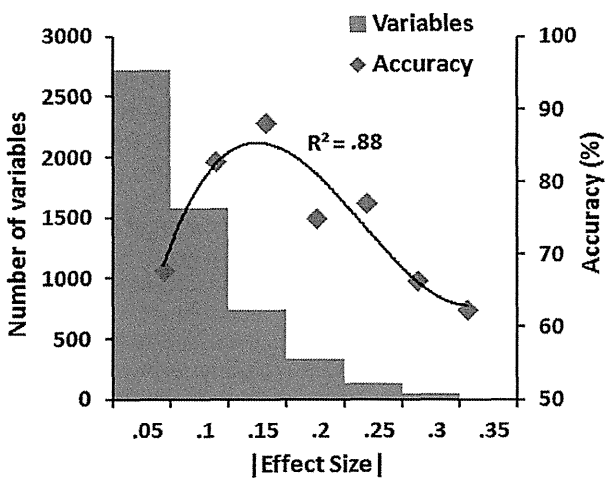

Fig. 3 – The vertical–left axis indicates the number of variables entered into the PNN and the vertical–right axis indicates the accuracy (%) of classification by the PNN. The horizontal axis indicates seven different ES thresholds. For example, at the threshold of ES = .1, the number of variables entered into PNN was 1,581, and the accuracy was 82.8%. The third degree polynomial regression line and r-square value for the accuracy data are shown.

The PNN classifier consists of four fully interconnected layers: an input layer, a pattern layer, a summation layer, and an output layer. The input layer has as many nodes as the number of features (i.e., number of cells in the matrix). The input layer nodes simply distribute input vectors to all the nodes in the pattern layer. The pattern layer has one node for each case in the training dataset (i.e., 640 cases or neurons). The pattern layer is fully connected to the input layer, with one node for each pattern in the datasets. Each node in the pattern layer receives the input vectors and estimates its probability density function, which was a Gaussian function in the present study. Here, a sigma value named as the "spread parameter" controls the size and shape of the Gaussian function. The optimal sigma values were estimated with the conjugate gradient algorithm. The jack-knife method was used for evaluating the sigma values during the optimization process. The pattern layer outputs are selectively connected to nodes in the summation layer depending on the class of patterns (i.e., ASD and CTL). There is one node for each class, and each node sums the outputs from the pattern layer nodes. The output layer node yields a binary output value corresponding to the best subclass choice for the specific dataset based on the maximum probability or Bayes' rule. Thus, the final product of the PNN is a value of 1 for one class and 0 for the other. In the present study, DTREG (http://www.dtreg.com) was used to run the PNN (Sherrod, 2003).

On the other hand, SVM performs classification by constructing a multidimensional hyperplane that separates the data into two categories (target variables). A set of features that describes one case is called a vector (i.e., predictor variables). Therefore, the goal of SVM modeling is to find the optimal hyperplane that separates clusters of vectors in such a way that cases with one category of the target variable are on one side of the plane and cases with the other category are on the other side of the plane. The vectors near the hyperplane are called support vectors. The distance between the support vectors is called the margin. An SVM analysis finds the hyperplane that maximizes the margin between the support vectors. In a high dimensional space, SVM uses a kernel function to map the data into a different space where a hyperplane can be used to separate the data (Sherrod, 2003). Several studies have found that PNN and SVM yielded comparable accuracy levels for classifying biological data (Loukas et al., 2013; Muniz et al., 2010); however, the PNN had advantages in the processing speed (Specht, 1990).

To explore an optimal set of feature variables, datasets at seven different ESs were entered individually into the PNN, and the prediction accuracy was computed by using leave-one-out cross-validation (LOOCV). In LOOCV, one subject's data are left out of the dataset, and the neural network creates an optimal classifier using the remaining data. The classifier predicts the label (ASD or CTL) of the one subject who was left out, and the accuracy of this prediction is assessed. This procedure was repeated as many times as the number of subjects, with a different subject being left out each time; finally, total accuracy was computed for each category. The prediction data included true positive (TP), false negative (FN), true negative (TN), and false positive (FP) classifications. The

sensitivity, specificity, accuracy, positive prediction value (PPV), and negative prediction value (NPV) were computed using the following formulas:

$$\text{Sensitivity} = TP/(TP + FN)*100$$

$$\text{Specificity} = TN/(TN + FP)*100$$

$$\text{Accuracy} = (TP + TN)/(TP + TN + FP + FN)*100$$

$$PPV = TP/(TP + FP)*100$$

$$NPV = TN/(TN + FN)*100$$

However, the PPV and NPV computed by the formulas above do not provide a realistic picture of the prediction value because they depend critically on the prevalence of the disorder in the general population (Castellanos, Di Martino, Craddock, Mehta, & Milham, 2013). Accordingly, these values were adjusted accounting for recent estimates of disorder prevalence from the Centers for Disease Control and Prevention, Morbidity and Mortality Weekly Report in 2012 (C.D.C.P., 2012). The corrected PPV and NPV were computed using the following formulas (Altman & Bland, 1994):

$$PPV_{corr} = \frac{\text{sensitivity}*\text{prevalence}}{\text{sensitivity}*\text{prevalence} + (1 - \text{specificity})*(1 - \text{prevalence})}$$

$$NPV_{corr} = \frac{\text{specificity}*(1 - \text{prevalence})}{\text{specificity}*(1 - \text{prevalence}) + (1 - \text{sensitivity})*\text{prevalence}}$$

The disease prevalence was .0113 according to the report noted above (C.D.C.P., 2012).

For the datasets at seven different ESs, the accuracy for the combined ASD and CTL groups was plotted in Fig. 3. Seven plots of accuracy data were fitted by a polynomial (3rd degree) function curve; consequently, it appeared that the optimal ES threshold existed within the range of .1–.2. Finally, the LOOCV procedure was repeated using datasets thresholded at absolute ES values ranging from .1 to .2 by .01 increments in an effort to determine the highest prediction accuracy. For the best prediction data, i.e., the dataset with the highest accuracy when the absolute value of ES was varied from .1 to .2, the ES (not the absolute value) matrix and lobar/region names are illustrated in Fig. 4.

2.4.3. *Other validation methods*

To confirm the reliability of the results of LOOCV, V-fold cross-validation (CV) of PNN was conducted by using the same correlation matrices of 640 subjects as those entered into the LOOCV. In a V-fold CV, a model was constructed with (V−1)/V proportion of the subjects being used. The selection of the subjects occurred randomly each time. The validation of a remaining set of subjects (1/V proportion of subjects) was performed using the constructed model. I conducted 2-, 10-, and 50-fold CVs. The validation results in each model are shown in Table 4.

2.5. *Effect of confounding factors*

2.5.1. *Effects of potentially confounding factors on accuracy*

Because the PNN was conducted on a dataset of 640 subjects from 12 institutes, variations of imaging and experimental protocols could artifactually alter the present results. To investigate whether the prediction accuracy was confounded by such factors, my accuracy data was compared across institutes, MRI vendors, eyes open/closed conditions, sex, age, handedness, and full-scale IQ groups (Fig. 5). For age, accuracy was compared among three groups (under 10 years old, $n = 119$; 10–15 years old, $n = 350$; and 15–20 years old, $n = 171$). For full-scale IQ values, the means ± 1 SD were used as cut-off points (under 91, $n = 105$; 92 to 121, $n = 417$; and over 122, $n = 115$). Chi-square tests were used for these analyses (statistical threshold was set at $p = .05$).

2.5.2. *Effects of medication and head movement on accuracy*

To investigate whether medication status affected prediction accuracy, chi-square tests were conducted for the three ASD groups (on-medication, off-medication, and no data). For analyzing the relationship between head movements and accuracy data, all 640 subjects were sorted according to the RMS value of head movement parameters and divided into 10 bins with 64 subjects each. The accuracy data was computed for each of the 10 bins and compared using chi-square tests. Data of x-translation and y-rotation were used for this analysis because significant group differences were obtained only for these two measures (see Results and Fig. 6). The statistical threshold of chi-square tests was set at $p = .05$.

2.5.3. *Characteristics of the false-negative group*

From a clinical point of view, the characteristics of subjects who had ASD but were incorrectly classified as having "typical development" (FN) are particularly important. Therefore, the proportion of sex and handedness, mean age, and mean and skewness of full-scale IQ were compared between the four classification groups (TP, FN, FP, and TN). In addition, the total score of ADOS (if ADOS was not available and total score of ADOS-Gotham was available, the latter was used) was compared between the TP (ADOS total score, 247 subjects; ADOS-Gotham total score, 23 subjects; no data, 17 subjects) and FN (ADOS total score, 18 subjects; ADOS-Gotham total score; 4 subjects; no data, 3 subjects) groups. For numerical variables other than skewness, one-way ANOVA was conducted (threshold was set at $p = .05$ after multiple comparisons with Fisher's least square method). The chi-square test was used to analyze the categorical variables (threshold was set at $p = .05$). These data are plotted in Fig. 7.